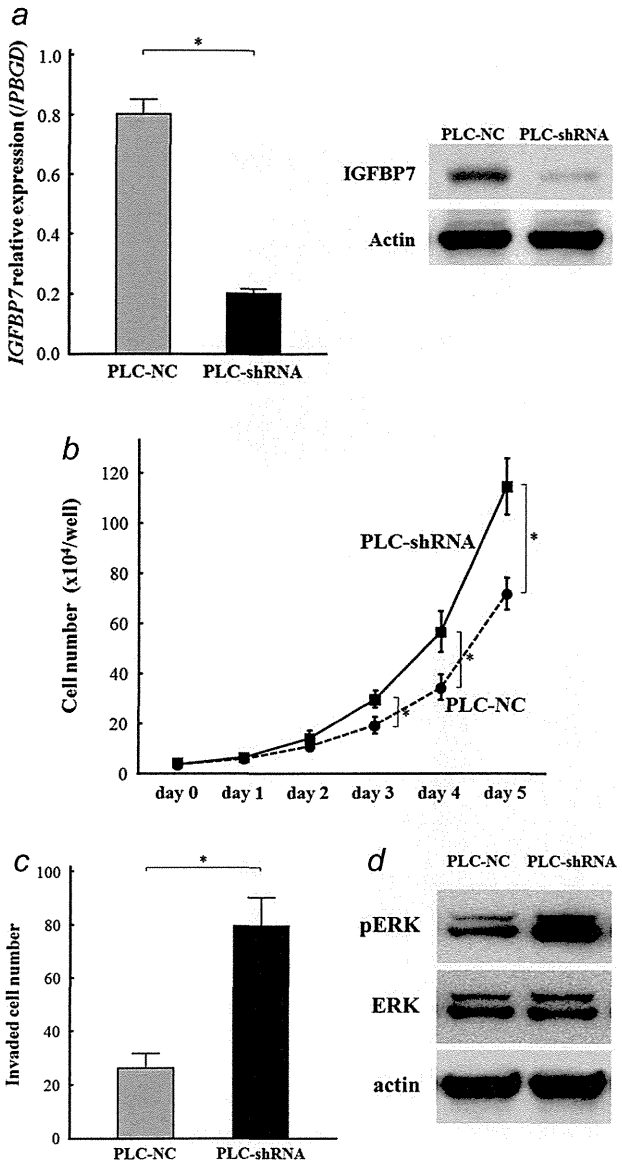

Figure 1. Characteristics of PLC/PRF/5 transfected with shRNA against *IGFBP7*. (*a*) qRT-PCR (Left panel) and western blot analysis (Right panel) indicated a significant decrease in IGFBP7 in cells transfected with shRNA compared to control cells (*$p < 0.05$). (*b*) Proliferation assays showed significantly quicker growth in the IGFBP7-suppressed cells compared with the control cells (*$p < 0.05$). (*c*) The invasion assay showed that the invasive ability of the IGFBP7-suppressed cells was significantly greater than that of the control cells (*$p < 0.05$). (*d*) Western blot analysis demonstrated significantly increased pERK expression in the IGFBP7-supperessed cells compared to the control cells. Data are mean ± SD of 3 experiments.

Immunohistochemical staining

Resected tissue samples were fixed in 10% buffered formalin and finally embedded in paraffin. Immunohistochemical staining for IGFBP7 in the same samples was performed as described previously.[17,20] Briefly, after deparaffinization and blocking, the sections were incubated overnight at 4°C with polyclonal goat anti-human IGFBP7 antibody, and then counterstained with Mayer's hematoxylin. IGFBP7 expression was defined as the presence of specific staining in the cytoplasm of cancer cells. IGFBP7 expression was evaluated as positive or negative, as previously prescribed.[17]

Statistical analysis

Data are expressed as mean ± SD. Differences between groups were assessed using the χ^2-test, and continuous variables were compared using Student's *t*-test. Survival rates were calculated according to the Kaplan-Meier method and compared using the log-rank test. Statistical analysis was performed using StatView (version 5.0; SAS Institute, Cary, NC). A p value < 0.05 was considered statistically significant.

Results

In vitro studies

IGFBP7 downregulation promotes proliferation and invasive activity. First, *IGFBP7* expression was examined by qRT-PCR in 4 HCC cell lines, PLC/PRF/5, HuH7, HLE and HepG2. The *IGFBP7* expression levels in PLC/PRF/5 and HuH7 were the highest and lowest of the 4 cell lines, respectively. A plasmid coding for shRNA against *IGFBP7* was then transfected into PLC/PRF/5, whose IGFBP7 expression level was the highest in the 4 cell lines. The IGFBP7 expression was suppressed by the transfection, as confirmed by qRT-PCR and western blot analysis (Fig. 1*a*). The proliferation assay showed significantly more rapid growth in the IGFBP7-suppressed cells compared to control cells (Fig. 1*b*). In addition, the invasive ability of the IGFBP7-suppressed cells was significantly greater than that of the control cells (Fig. 1*c*). Based on previous studies that IGFBP7 downregulation promotes cell proliferation through ERK signaling, we analyzed the levels of total ERK and pERK in our cells.[10,21] pERK expression was significantly increased in the IGFBP7-supperessed cells, while total ERK expression was not changed, which coincided with previous reports (Fig. 1*d*). On the other hand, as we previously reported, there were no significant differences in the expression of total Akt or phoshorylated Akt between the IGFBP7-supperessed cells and the control cells.[17]

Downregulation of IGFBP7 attenuates apoptosis. The extent of apoptosis of these cells was examined by the Annexin V assay. The percentages of early apoptotic cells and late apoptotic cells defined by Annexin V-positive/PI-negative cells and Annexin V-positive/PI-positive cells respectively were significantly lower in the IGFBP7-suppressed cells than those in the control cells (Fig. 2*a*).[22] This significant difference of the extent of apoptosis was also confirmed under the condition where apoptosis is induced by some agents, which was reported previously.[17] Next, the expression of proteins related to apoptosis was examined. The result showed that cleaved caspase-3 and cleaved PARP are significantly decreased in

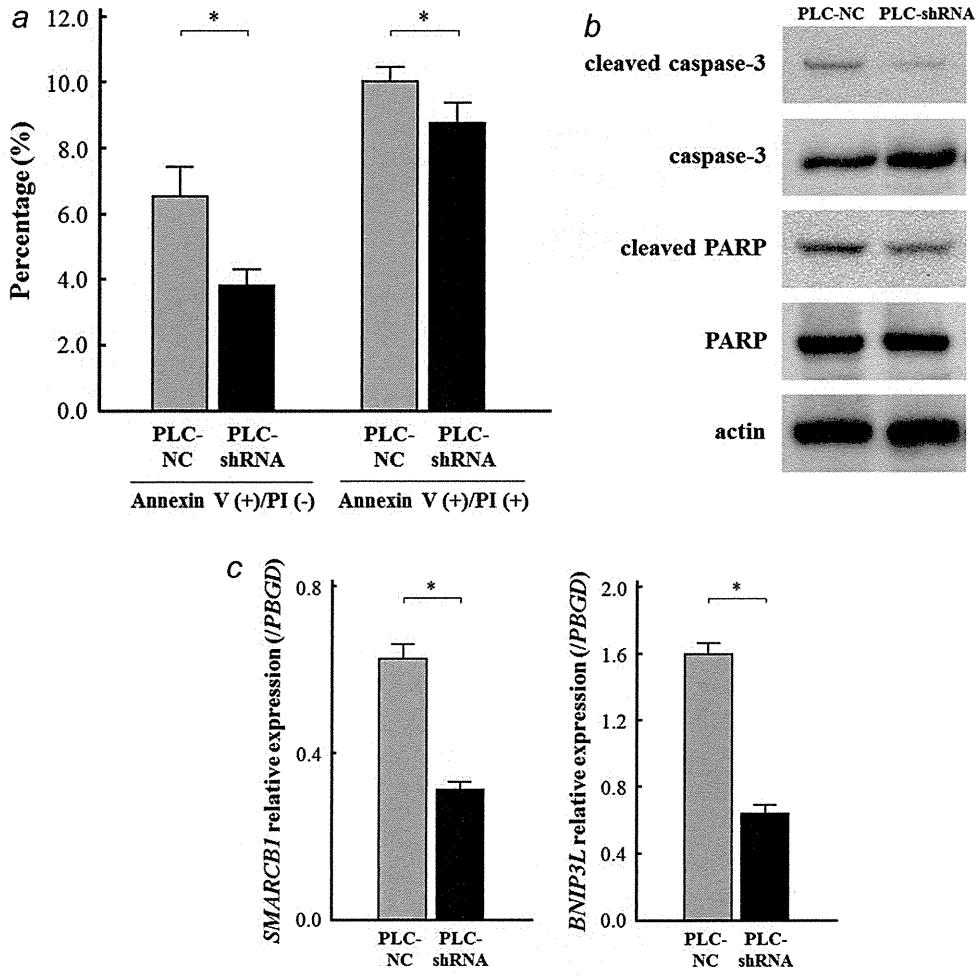

Figure 2. The extent of apoptosis evaluated by the amount of apoptotic cells and the expression of apoptosis-related molecules. (*a*) The Annexin V assay showed the percentage of cells in early apoptosis and in late apoptosis defined by Annexin V-positive/PI-negative cells and Annexin V-positive/PI-positive cells respectively were significantly lower in the IGFBP7-suppressed cells than the control cells (*$p < 0.05$). (*b*) Cleaved caspase-3 and cleaved PARP were decreased in the IGFBP7-suppressed cells. (*c*) qRT-PCR indicated that *SMARCB1* (Left panel) and *BNIP3L* (Right panel) expression levels were significantly decreased in the IGFBP7-supressed cells than the control cells (*$p < 0.05$). Data are mean ± SD of 3 experiments.

the IGFBP7-suppressed cells, while total caspase-3 and PARP expressions were not changed (Fig. 2*b*). In addition, since apoptosis induced by IGFBP7 was reported to occur *via* SMARCB1 and BNIP3L upregulation, we also evaluated the expression levels of *SMARCB1* and *BNIP3L* by qRT-PCR.[10] The results showed that *SMARCB1* and *BNIP3L* expressions were significantly decreased in the IGFBP7-supressed cells compared with the control cells (Fig. 2*c*).

Downregulation of IGFBP7 promotes cell cycle progression. The influence of IGFBP7 on cell cycle was examined by flow cytometric analysis. Prior to the examination, cells were synchronized in the G_0/G_1 phase by serum starvation for 72 hr, and then put back in the regular medium with 10% fetal bovine serum. Dynamic changes in percentage between G_0/G_1 phase and S phase are shown in Figure 3*a*. The proportion of G_0/G_1 phase and S phase on the end of the starvation (0 hr) was almost comparable between the IGFBP7-suppressed cells and the control cells. As shown in Figure 4, the time with minimum percentage of G_0/G_1 phase and maximum percentage of S phase was 24 hr in the control cells, while the time was 12 hr in the IGFBP7-suppressed cells, which suggests that the cell cycle progression was more rapid in the IGFBP7-suppressed cells than that in the control cells. Furthermore, we found that cyclin D1 and cyclin E were increased and p27 was decreased in the IGFBP7-suppressed cells than those in the control cells, and that there was no significant difference in p21 expression between the 2 cells, which was agreement with more rapid cell cycle progression in the IGFBP7-suppressed cells (Fig. 3*b*).

Transfection of IGFBP7 attenuates proliferation and invasive activity. Next, the *IGFBP7* expression plasmid was transfected into HuH7, whose IGFBP7 expression level was the lowest in the 4 HCC cell lines. The IGFBP7 expression was increased by

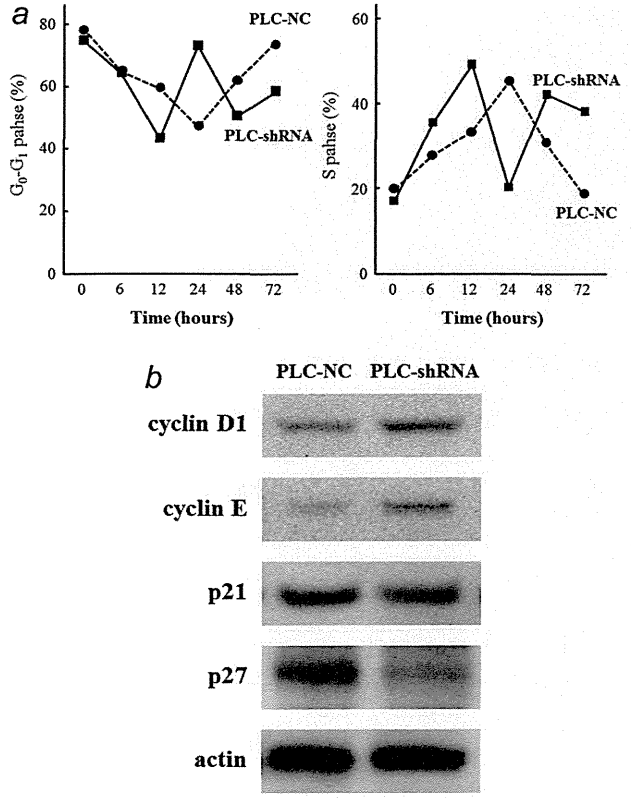

Figure 3. Cell cycle progression assessed by a flow cytometric analysis and the expression of cell cycle-related molecules. (*a*) Time with minimum percentage of G_0/G_1 phase (Left panel) and maximum percentage of S phase (Right panel) was 24 hr and 12 hr in the control cells and the IGFBP7-suppressed cells, respectively. (*b*) Cyclin D1 and cyclin E were increased and p27 was decreased in the IGFBP7-suppressed cells than the control cells, and there was no significant difference in p21 expression between the 2 cells.

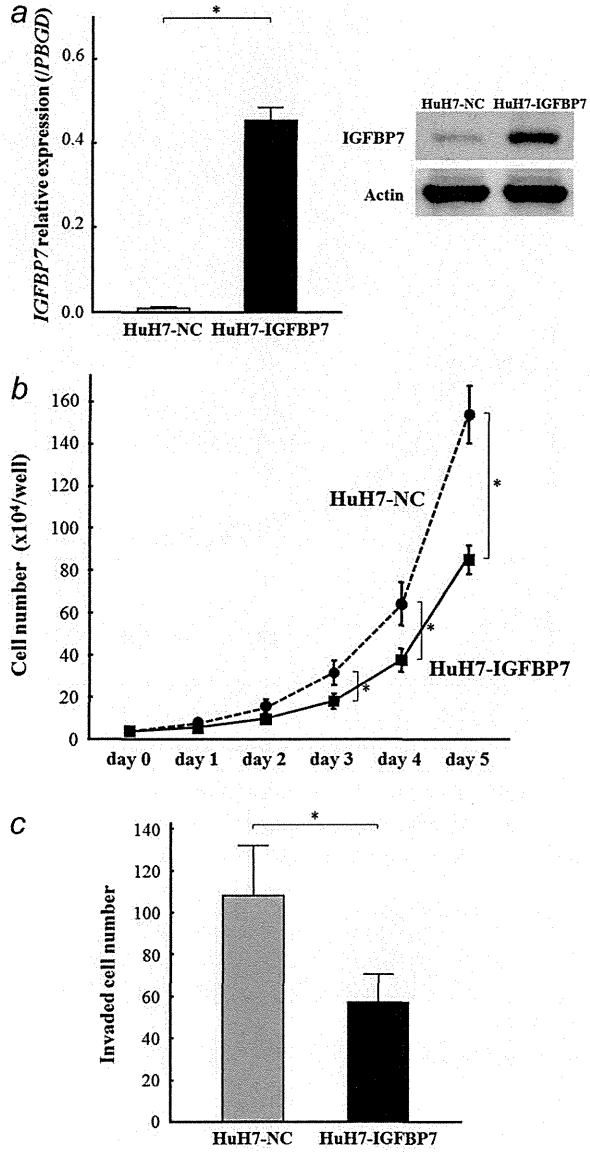

Figure 4. Characteristics of HuH7 transfected with *IGFBP7* expression plasmid. (*a*) qRT-PCR (Left panel) and western blot analysis (Right panel) indicated a significant increase in IGFBP7 in cells transfected with *IGFBP7* expression plasmid compared with control cells (*$p < 0.05$). (*b*) Proliferation assays showed significantly slower growth in the IGFBP7-overexpressing cells compared to the control cells (*$p < 0.05$). (*c*) The invasion assay showed that the invasive ability of the IGFBP7-overexpressing cells was significantly weaker than that of the control cells (*$p < 0.05$). Data are mean ± SD of 3 experiments.

the transfection, as confirmed by qRT-PCR and western blot analysis (Fig. 4*a*). The proliferation assay showed significantly less rapid growth in the IGFBP7-overexpressing cells compared to the control cells (Fig. 4*b*). In addition, the invasive ability of the IGFBP7-overexpressing cells was significantly weaker than that of the control cells (Fig. 4*c*), which were consistent to the results of the above shRNA plasmid experiments.

In vivo studies

IGFBP7 expression correlates with tumor-related factors in clinical HCC samples.. Next, IGFBP7 expression in the tumoral leison was evaluated in clinical sample by immunohistochemical staining. The immunohistochemical analysis showed that among the 104 patients examined, 67 patients (64.4%) showed positive staining for IGFBP7 and the remaining 37 patients (35.6%) were negative for IGFBP7. The immunohistochemical findings of representative cases are shown in Figure 5*a*. The clinicopathological factors related to IGFBP7 expression status of the 104 patients are summarized in Table 1. The data indicated that IGFBP7 expression was significantly associated with maximum tumor size and vascular invasion ($p < 0.0001$, $p = 0.0095$, respectively).

On the other hand, the IGFBP7 expression in nontumoral lesion was homogenously observed in the cytoplasm of cells in all the 104 patients. The immunohistochemically

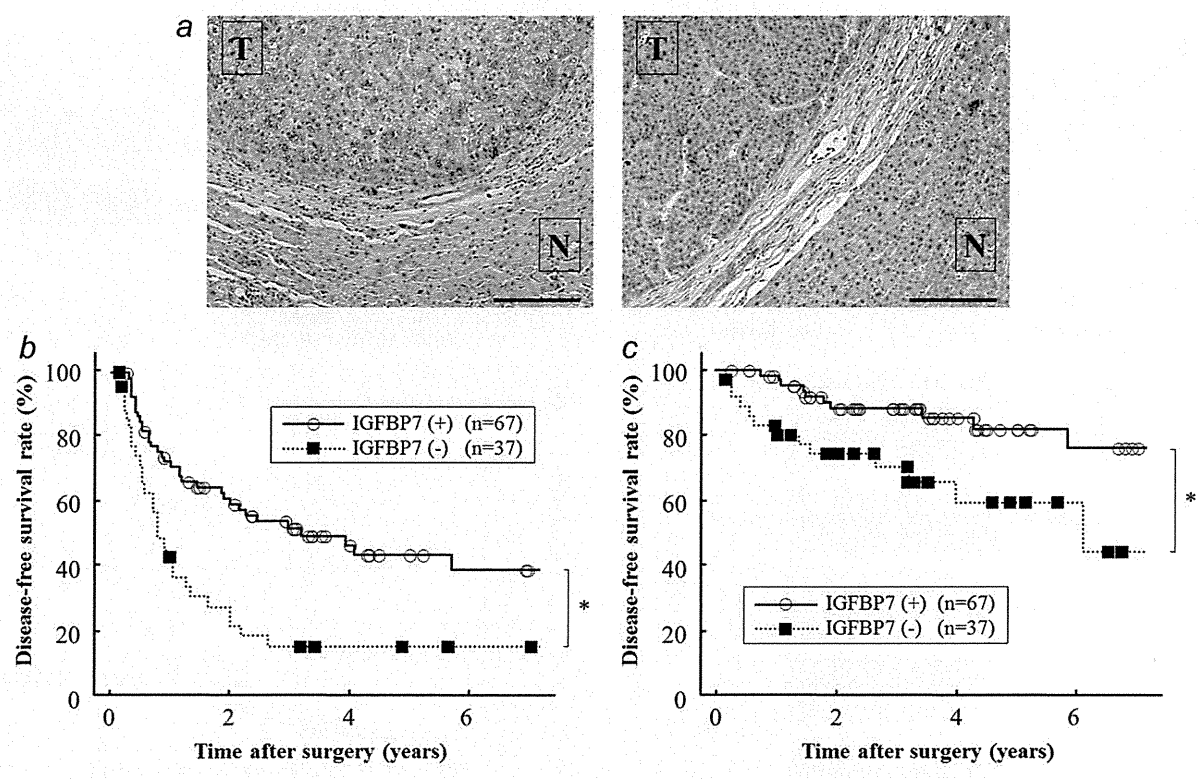

Figure 5. IGFBP7 expression and postoperative outcome in HCC patients. (*a*) Immunohistochemical findings in representative positive case (Left panel) and negative case (Right panel). T, tumoral lesion; N, non-tumoral lesion. Bar = 200 μm. Disease-free survival (*b*) and overall survival (*c*) in patients negative for IGFBP7 expression were significantly poorer than in cells expressing IGFBP7 (*$p < 0.05$).

Table 1. Clinicopathological characteristics of patients with HCC according to IGFBP7 status

	IFGFBP7 (+) (n = 67)	IGFBP7 (−) (n = 37)	p-value
Clinical factors			
Gender (male/female)	53/14	29/8	0.9308
Age (years)[1]	65 ± 10	63 ± 10	0.3900
HBs-Ag (−/+)	52/15	30/7	0.6783
Anti-HCV Ab (−/+)	29/38	15/22	0.7863
Child-Pugh classification (A/B)	58/9	29/8	0.2796
Liver cirrhosis (−/+)	31/36	20/17	0.4470
Tumor-related factors			
AFP (ng/ml)[1]	15,155 ± 122,143	30,243 ± 86,058	0.5075
PIVKA-II (mAU/ml)[1]	26,656 ± 87,446	151,639 ± 1,221,431	0.5365
Number of tumors (single/multiple)	47/20	21/16	0.1693
Maximum tumor size (cm)	3.2 ± 1.7	6.5 ± 4.7	<0.0001
Vascular invasion (−/+)	58/9	24/13	0.0095
Edmondson-Steiner grade (I,II/III,IV)	31/36	11/26	0.0998

[1]Data are expressed as mean ± SD.
Abbreviations: IGFBP7, insulin-like growth factor binding protein 7; HBs-Ag, hepatitis B surface antigen; Anti-HCV Ab, anti-hepatic C virus antibody; AFP:, alpha-fetoprotein; PIVKA-II, protein induced by vitamin K absence or antagonists-II.

determined IGFBP7 expression level was similar between 53 cirrhotic patients and the remaining 51 non-cirrhotic patients.

IGFBP7 downregulation is an independent significant predictor for postoperative outcome in HCC patients. The disease-free survival (DFS) in patients without IGFBP7 expression (1-/

Table 2. Statistical analysis of disease-free survival and overall survival of patients with HCC

	Disease-free survival				Overall survival			
	Univariate	Multivariate			Univariate	Multivariate		
	p-value	OR	95% CI	*p*-value	*p*-value	OR	95% CI	*p*-value
Clinical factors								
Gender (male/female)	0.2192				0.1968			
Age (years) (≤64/>64)	0.5542				0.8018			
HBs-Ag (−/+)	0.2440				0.3605			
Anti-HCV Ab (−/+)	0.9405				0.5034			
Child-Pugh classification (A/B)	0.2586				0.7501			
Liver cirrhosis (−/+)	0.1429				0.5587			
Tumor-related factors								
AFP (ng/ml) (≤400/>400)	0.0629				0.1042			
PIVKA-II (mAU/ml) (≤40/>40)	0.2912				0.1563			
Number of tumors (single/multiple)	0.0025	1.659	0.978–2.815	0.0604	0.0007	2.288	0.905–5.780	0.0801
Maximum tumor size (cm) (≤5/>5)	0.0001	1.387	0.737–2.611	0.3100	0.0290	1.512	0.579–3.949	0.3991
Vascular invasion (−/+)	<0.0001	2.681	1.400–5.135	0.0029	<0.0001	4.649	1.705–12.679	0.0027
Edmondson-Steiner grade (I,II/III,IV)	0.0392	1.520	0.894–2.574	0.1225	0.0180	5.587	1.616–19.231	0.0066
IGFBP7 status (−/+)	0.0007	1.919	1.112–3.313	0.0192	0.0063	2.659	1.102–6.418	0.0296

Abbreviations: IGFBP7, insulin-like growth factor binding protein 7; HBs-Ag, hepatitis B surface antigen; Anti-HCV Ab, anti-hepatic C virus antibody; AFP:, alpha-fetoprotein; PIVKA-II, protein induced by vitamin K absence or antagonists-II; OR, odds ratio; 95% CI, 95% confidence interval.

3-/5-year: 42.9%/15.3%/15.3%) was significantly poorer than that in patients showing IGFBP7 expression (1-/3-/5-year: 70.9%/51.8%/43.6%) ($p = 0.0002$; Fig. 5*b*). Univariate analyses showed that number of tumors ($p = 0.0025$), maximum tumor size ($p = 0.0001$), presence/absence of vascular invasion ($p < 0.0001$), and Edmondson-Steiner grade ($p = 0.0392$) all significantly correlated with DFS, in addition to IGFBP7 status (Table 2). Multivariate analysis for DFS using the above 5 factors identified presence/absence of vascular invasion and IGFBP7 status as independent significant factors (Table 2).

The overall survival (OS) rate in patients without IGFBP7 expression (1-/3-/5-year: 83.4%/70.2%/59.2%) was also significantly lower than that in patients with positive IGFBP7 expression (1-/3-/5-year: 98.5%/88.4%/82.0%) ($p = 0.0063$; Fig. 5*c*). By univariate analysis, number of tumors ($p = 0.0007$), maximum tumor size ($p = 0.0290$), presence/absence of vascular invasion ($p < 0.0001$), and Edmondson-Steiner grade ($p = 0.0180$) were also significantly correlated with OS (Table 2). Multivariate analysis using the above 5 factors identified presence/absence of vascular invasion, Edmondson-Steiner grade, and IGFBP7 status as independent significant factors in OS (Table 2). Thus, IGFBP7 expression was an overall independent significant factor for postoperative prognosis in HCC patients.

Discussion

In this study, we first analyzed IGFBP7 function *in vitro* experiments. The results demonstrated that IGFBP7 downregulation was significantly associated with rapid growth and proliferation of HCC cells. In addition, the cells showed decreased apoptotic cell numbers and expression of apoptosis-related proteins, enhancement of ERK signaling, and rapid cell cycle progression. Considering the implicated tumor suppression activity of IGFBP7, the results of this study are consistent with previous similar reports.[7,9–11,14,15,21] We also previously reported a significant association of IGFBP7 downregulation with resistance to some chemotherapeutic drugs in HCC cells.[17] Taken together, it seems apparent that IGFBP7 downregulation is significantly associated with the malignant potential of cancer cells including proliferation, invasiveness, and resistance to chemotherapeutic drugs. To our knowledge, this is the first study to examine the functional role of IGFBP7 in HCC. On the other hand, the cause-and-effect relationship between the IGFBP7 downregulation and the malignant potential is still unsolved, which is expected to be elucidated by further studies in future.

This study also assessed the prognostic significance of IGFBP7 expression in resected human HCC samples. From these findings, IGFBP7 downregulation was significantly associated with tumor progression and postoperative poor prognosis in our patients group, and IGFBP7 status was identified as an independent significant prognostic factor, in addition to other well-known factors. This finding was consistent with the results of the *in vitro* experiments and serves to suggest that assessing the IGFBP7 expression status of patients with HCC could improve the prediction of prognosis.

We have reported some studies of significant prognostic predictors after surgery for HCC.[20,23–38] In one of the studies, based on cDNA microarray analysis, we identified a set of multiple genes whose expressions were significantly different

between patients with good prognosis and those with poor prognosis, and revealed that the gene set was one of the independent prognostic factors.[38] IGFBP7 was not included in the gene set because the difference of the expression level was not large between the 2 groups, but the IGFBP7 expression level examined by the microarray analysis was also significantly correlated to the prognosis. This result seems to be consistent with the result of this study. In addition, considering the significant inverse correlation of IGFBP7 expression to the extent of apoptosis and cell cycle progression confirmed by the *in vitro* experiments, our previous reports of apoptosis- and cell cycle-related molecules as prognostic factors are in agreement with the prognostic impact of IGFBP7.[25,26,34,35] Furthermore, we have reported that angiogenesis-related molecules such as angiopoietin-2 and hypoxia-induced factor-1α are significant factors for postoperative prognosis.[33] Considering that IGFBP7 was reported to block angiogenesis in human vascular endothelial cells, it may be possible that there is a significant correlation between IGFBP7 expression and the angiogenesis-related molecules, though we did not examine it in this study.[39]

IGFBP7 is a secreted protein, and recombinant IGFBP7 is commonly purified.[40,41] Indeed, previous studies of IGFBP7 function have expressed the protein exogenously using IGFBP7 viral vectors or by administering recombinant protein.[39] In addition, IGFBP7 has also been studied as a possible therapeutic agent for treatment of malignancies that are dependent on BRAF-MEK-ERK signaling.[10,42] Thus, recombinant IGFBP7 could be potentially suitable therapeutically to improve the poor prognosis of HCC patients lacking IGFBP7 expression. In addition, IGFBP7 expression is also subject to epigenetic modification, and aberrant methylation of CpG islands in the *IGFBP7* promoter region was confirmed in several kinds of cancers.[10,43] In this regard, Wajapeyee *et al.*[10] showed that treatment of melanoma cell lines with DNA methyltransferase inhibitor, 5-aza-2′-deoxycytidine, restored IGFBP7 expression. Such a finding suggests a therapeutic application whereby IGFBP7 expression and thus function are restored using a DNA methyltransferase inhibitor. Exploring these therapeutic interventions against HCC was unfortunately beyond the scope of this study, and further studies are definitely needed in this regard.

In summary, we found that IGFBP7 downregulation was significantly associated with both tumor progression and clinical outcome in HCC. This result suggested that analysis of IGFBP7 expression in patients might help to predict prognosis, and that IGFBP7 could be a novel therapeutic target in HCC patients with poor prognosis.

References

1. Block TM, Mehta AS, Fimmel CJ, Jordan R. Molecular viral oncology of hepatocellular carcinoma. *Oncogene* 2003; 22:5093–107.
2. Bosch FX, Ribes J, Diaz M, Cleries R. Primary liver cancer: worldwide incidence and trends. *Gastroenterology* 2004;127: S5–S16.
3. Zhu AX. Systemic therapy of advanced hepatocellular carcinoma: how hopeful should we be? *Oncologist* 2006;11:790–800.
4. Tung-Ping Poon R, Fan ST, Wong J. Risk factors, prevention, and management of postoperative recurrence after resection of hepatocellular carcinoma. *Ann Surg* 2000; 232:10–24.
5. Zhao WH, Ma ZM, Zhou XR, Feng YZ, Fang BS. Prediction of recurrence and prognosis in patients with hepatocellular carcinoma after resection by use of CLIP score. *World J Gastroenterol* 2002;8:237–42.
6. Zhou J, Tang ZY, Wu ZQ, Zhou XD, Ma ZC, Tan CJ, Shi YH, Yu Y, Qiu SJ, Fan J. Factors influencing survival in hepatocellular carcinoma patients with macroscopic portal vein tumor thrombosis after surgery, with special reference to time dependency: a single-center experience of 381 cases. *Hepatogastroenterology* 2006;53: 275–80.
7. Mutaguchi K, Yasumoto H, Mita K, Matsubara A, Shiina H, Igawa M, Dahiya R, Usui T. Restoration of insulin-like growth factor binding protein-related protein 1 has a tumor-suppressive activity through induction of apoptosis in human prostate cancer. *Cancer Res* 2003;63: 7717–23.
8. Sato Y, Chen Z, Miyazaki K. Strong suppression of tumor growth by insulin-like growth factor-binding protein-related protein 1/tumor-derived cell adhesion factor/mac25. *Cancer Sci* 2007;98:1055–63.
9. Kato MV. A secreted tumor-suppressor, mac25, with activin-binding activity. *Mol Med* 2000;6:126–35.
10. Wajapeyee N, Serra RW, Zhu X, Mahalingam M, Green MR. Oncogenic BRAF induces senescence and apoptosis through pathways mediated by the secreted protein IGFBP7. *Cell* 2008;132:363–74.
11. Wilson HM, Birnbaum RS, Poot M, Quinn LS, Swisshelm K. Insulin-like growth factor binding protein-related protein 1 inhibits proliferation of MCF-7 breast cancer cells via a senescence-like mechanism. *Cell Growth Differ* 2002;13:205–13.
12. Lin J, Lai M, Huang Q, Ruan W, Ma Y, Cui J. Reactivation of IGFBP7 by DNA demethylation inhibits human colon cancer cell growth in vitro. *Cancer Biol Ther* 2008; 7:1896–900.
13. Burger AM, Zhang X, Li H, Ostrowski JL, Beatty B, Venanzoni M, Papas T, Seth A. Down-regulation of T1A12/mac25, a novel insulin-like growth factor binding protein related gene, is associated with disease progression in breast carcinomas. *Oncogene* 1998;16:2459–67.
14. Landberg G, Ostlund H, Nielsen NH, Roos G, Emdin S, Burger AM, Seth A. Downregulation of the potential suppressor gene IGFBP-rP1 in human breast cancer is associated with inactivation of the retinoblastoma protein, cyclin E overexpression and increased proliferation in estrogen receptor negative tumors. *Oncogene* 2001;20:3497–505.
15. Ruan WJ, Lin J, Xu EP, Xu FY, Ma Y, Deng H, Huang Q, Lv BJ, Hu H, Cui J, Di MJ, Dong JK, et al. IGFBP7 plays a potential tumor suppressor role against colorectal carcinogenesis with its expression associated with DNA hypomethylation of exon 1. *J Zhejiang Univ Sci B* 2006;7:929–32.
16. Kondo M, Nagano H, Wada H, Damdinsuren B, Yamamoto H, Hiraoka N, Eguchi H, Miyamoto A, Yamamoto T, Ota H, Nakamura M, Marubashi S, et al. Combination of IFN-alpha and 5-fluorouracil induces apoptosis through IFN-alpha/beta receptor in human hepatocellular carcinoma cells. *Clin Cancer Res* 2005;11:1277–86.
17. Tomimaru Y, Eguchi H, Wada H, Noda T, Murakami M, Kobayashi S, Marubashi S, Takeda Y, Tanemura M, Umeshita K, Doki Y, Mori M, et al. Insulin-like growth

factor-binding protein 7 alters the sensitivity to interferon-based anticancer therapy in hepatocellular carcinoma cells. *Br J Cancer* 2010;102:1483–90.
18. Nakamura M, Nagano H, Sakon M, Yamamoto T, Ota H, Wada H, Damdinsuren B, Noda T, Marubashi S, Miyamoto A, Takeda Y, Umeshita K, et al. Role of the Fas/FasL pathway in combination therapy with interferon-alpha and fluorouracil against hepatocellular carcinoma in vitro. *J Hepatol* 2007;46:77–88.
19. Eguchi H, Nagano H, Yamamoto H, Miyamoto A, Kondo M, Dono K, Nakamori S, Umeshita K, Sakon M, Monden M. Augmentation of antitumor activity of 5-fluorouracil by interferon alpha is associated with up-regulation of p27Kip1 in human hepatocellular carcinoma cells. *Clin Cancer Res* 2000;6: 2881–90.
20. Kondo M, Yamamoto H, Nagano H, Okami J, Ito Y, Shimizu J, Eguchi H, Miyamoto A, Dono K, Umeshita K, Matsuura N, Wakasa K, et al. Increased expression of COX-2 in nontumor liver tissue is associated with shorter disease-free survival in patients with hepatocellular carcinoma. *Clin Cancer Res* 1999;5:4005–12.
21. Vizioli MG, Sensi M, Miranda C, Cleris L, Formelli F, Anania MC, Pierotti MA, Greco A. IGFBP7: an oncosuppressor gene in thyroid carcinogenesis. *Oncogene* 2010; 29:3835–44.
22. Lugli E, Troiano L, Ferraresi R, Roat E, Prada N, Nasi M, Pinti M, Cooper EL, Cossarizza A. Characterization of cells with different mitochondrial membrane potential during apoptosis. *Cytometry A* 2005;68:28–35.
23. Arai I, Nagano H, Kondo M, Yamamoto H, Hiraoka N, Sugita Y, Ota H, Yoshioka S, Nakamura M, Wada H, Damdinsuren B, Kato H, et al. Overexpression of MT3-MMP in hepatocellular carcinoma correlates with capsular invasion. *Hepatogastroenterology* 2007;54:167–71.
24. Damdinsuren B, Nagano H, Kondo M, Yamamoto H, Hiraoka N, Yamamoto T, Marubashi S, Miyamoto A, Umeshita K, Dono K, Nakamori S, Wakasa K, et al. Expression of Id proteins in human hepatocellular carcinoma: relevance to tumor dedifferentiation. *Int J Oncol* 2005; 26:319–27.
25. Ito Y, Matsuura N, Sakon M, Miyoshi E, Noda K, Takeda T, Umeshita K, Nagano H, Nakamori S, Dono K, Tsujimoto M, Nakahara M, et al. Expression and prognostic roles of the G1-S modulators in hepatocellular carcinoma: p27 independently predicts the recurrence. *Hepatology* 1999;30:90–9.
26. Ito Y, Matsuura N, Sakon M, Takeda T, Umeshita K, Nagano H, Nakamori S, Dono K, Tsujimoto M, Nakahara M, Nakao K, Monden M. Both cell proliferation and apoptosis significantly predict shortened disease-free survival in hepatocellular carcinoma. *Br J Cancer* 1999;81:747–51.
27. Kittaka N, Takemasa I, Seno S, Takeda Y, Kobayashi S, Marubashi S, Dono K, Umeshita K, Nagano H, Matsuda H, Monden M, Mori M, et al. Exploration of potential genomic portraits associated with intrahepatic recurrence in human hepatocellular carcinoma. *Ann Surg Oncol* 2010;17:3145–54.
28. Kittaka N, Takemasa I, Takeda Y, Marubashi S, Nagano H, Umeshita K, Dono K, Matsubara K, Matsuura N, Monden M. Molecular mapping of human hepatocellular carcinoma provides deeper biological insight from genomic data. *Eur J Cancer* 2008;44:885–97.
29. Miyamoto A, Nagano H, Sakon M, Fujiwara Y, Sugita Y, Eguchi H, Kondo M, Arai I, Morimoto O, Dono K, Umeshita K, Nakamori S, et al. Clinical application of quantitative analysis for detection of hematogenous spread of hepatocellular carcinoma by real-time PCR. *Int J Oncol* 2001;18:527–32.
30. Morimoto O, Nagano H, Sakon M, Fujiwara Y, Yamada T, Nakagawa H, Miyamoto A, Kondo M, Arai I, Yamamoto T, Ota H, Dono K, et al. Diagnosis of intrahepatic metastasis and multicentric carcinogenesis by microsatellite loss of heterozygosity in patients with multiple and recurrent hepatocellular carcinomas. *J Hepatol* 2003;39:215–21.
31. Noda T, Nagano H, Tomimaru Y, Murakami M, Wada H, Kobayashi S, Marubashi S, Eguchi H, Takeda Y, Tanemura M, Umeshita K, Kim T, et al. Prognosis of hepatocellular carcinoma with biliary tumor thrombi following liver surgery. *Surgery* 2011;149:371–7.
32. Sakon M, Umeshita K, Nagano H, Eguchi H, Kishimoto S, Miyamoto A, Ohshima S, Dono K, Nakamori S, Gotoh M, Monden M. Clinical significance of hepatic resection in hepatocellular carcinoma: analysis by disease-free survival curves. *Arch Surg* 2000;135:1456–9.
33. Wada H, Nagano H, Yamamoto H, Yang Y, Kondo M, Ota H, Nakamura M, Yoshioka S, Kato H, Damdinsuren B, Tang D, Marubashi S, et al. Expression pattern of angiogenic factors and prognosis after hepatic resection in hepatocellular carcinoma: importance of angiopoietin-2 and hypoxia-induced factor-1 alpha. *Liver Int* 2006;26:414–23.
34. Xu X, Yamamoto H, Sakon M, Yasui M, Ngan CY, Fukunaga H, Morita T, Ogawa M, Nagano H, Nakamori S, Sekimoto M, Matsuura N, et al. Overexpression of CDC25A phosphatase is associated with hypergrowth activity and poor prognosis of human hepatocellular carcinomas. *Clin Cancer Res* 2003;9:1764–72.
35. Xu X, Sakon M, Nagano H, Hiraoka N, Yamamoto H, Hayashi N, Dono K, Nakamori S, Umeshita K, Ito Y, Matsuura N, Monden M. Akt2 expression correlates with prognosis of human hepatocellular carcinoma. *Oncol Rep* 2004; 11:25–32.
36. Yamamoto S, Tomita Y, Nakamori S, Hoshida Y, Nagano H, Dono K, Umeshita K, Sakon M, Monden M, Aozasa K. Elevated expression of valosin-containing protein (p97) in hepatocellular carcinoma is correlated with increased incidence of tumor recurrence. *J Clin Oncol* 2003;21: 447–52.
37. Yang Y, Nagano H, Ota H, Morimoto O, Nakamura M, Wada H, Noda T, Damdinsuren B, Marubashi S, Miyamoto A, Takeda Y, Dono K, et al. Patterns and clinicopathologic features of extrahepatic recurrence of hepatocellular carcinoma after curative resection. *Surgery* 2007;141: 196–202.
38. Yoshioka S, Takemasa I, Nagano H, Kittaka N, Noda T, Wada H, Kobayashi S, Marubashi S, Takeda Y, Umeshita K, Dono K, Matsubara K, et al. Molecular prediction of early recurrence after resection of hepatocellular carcinoma. *Eur J Cancer* 2009;45:881–9.
39. Tamura K, Hashimoto K, Suzuki K, Yoshie M, Kutsukake M, Sakurai T. Insulin-like growth factor binding protein-7 (IGFBP7) blocks vascular endothelial cell growth factor (VEGF)-induced angiogenesis in human vascular endothelial cells. *Eur J Pharmacol* 2009;610:61–7.
40. Akaogi K, Okabe Y, Sato J, Nagashima Y, Yasumitsu H, Sugahara K, Miyazaki K. Specific accumulation of tumor-derived adhesion factor in tumor blood vessels and in capillary tube-like structures of cultured vascular endothelial cells. *Proc Natl Acad Sci USA* 1996;93:8384–9.
41. Oh Y, Nagalla SR, Yamanaka Y, Kim HS, Wilson E, Rosenfeld RG. Synthesis and characterization of insulin-like growth factor-binding protein (IGFBP)-7. Recombinant human mac25 protein specifically binds. IGF-I and -II. *J Biol Chem* 1996;271:30322–5.
42. Wajapeyee N, Kapoor V, Mahalingam M, Green MR. Efficacy of IGFBP7 for treatment of metastatic melanoma and other cancers in mouse models and human cell lines. *Mol Cancer Ther* 2009;8:3009–14.
43. Lin J, Lai M, Huang Q, Ma Y, Cui J, Ruan W. Methylation patterns of IGFBP7 in colon cancer cell lines are associated with levels of gene expression. *J Pathol* 2007; 212:83–90.

Provided for non-commercial research and education use.
Not for reproduction, distribution or commercial use.

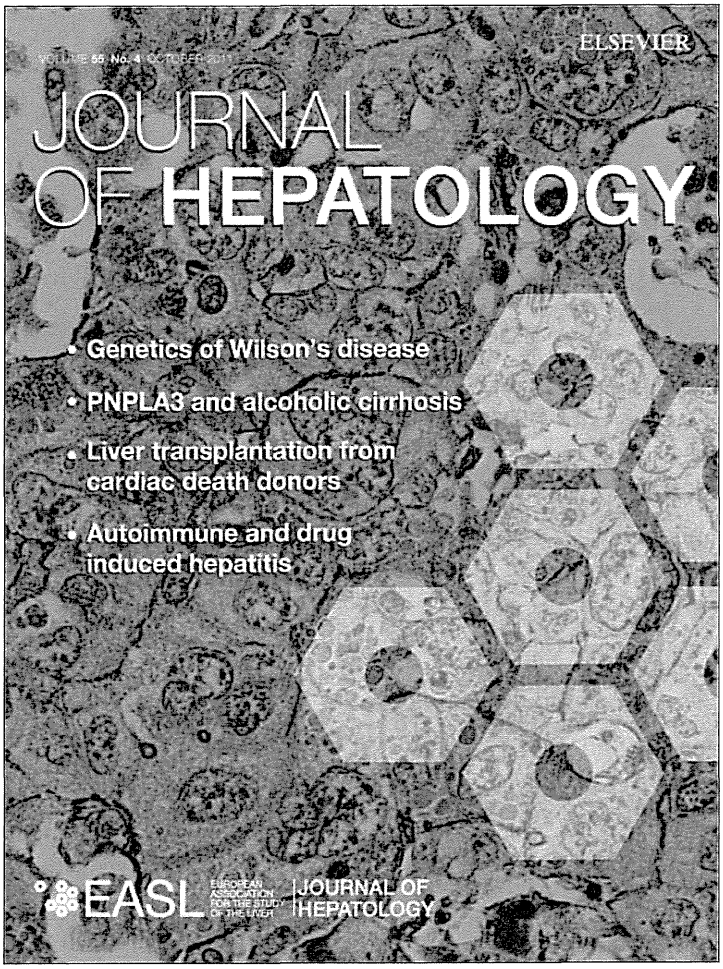

This article appeared in a journal published by Elsevier. The attached copy is furnished to the author for internal non-commercial research and education use, including for instruction at the authors institution and sharing with colleagues.

Other uses, including reproduction and distribution, or selling or licensing copies, or posting to personal, institutional or third party websites are prohibited.

In most cases authors are permitted to post their version of the article (e.g. in Word or Tex form) to their personal website or institutional repository. Authors requiring further information regarding Elsevier's archiving and manuscript policies are encouraged to visit:

http://www.elsevier.com/copyright

Author's personal copy

Research Article

EASL EUROPEAN ASSOCIATION FOR THE STUDY OF THE LIVER | JOURNAL OF HEPATOLOGY

Proliferative activity in hepatocellular carcinoma is closely correlated with glucose metabolism but not angiogenesis

Koji Kitamura[1], Etsuro Hatano[1,*], Tatsuya Higashi[2], Masato Narita[1], Satoru Seo[3], Yuji Nakamoto[4], Kenya Yamanaka[1], Hiromitsu Nagata[1], Kojiro Taura[1], Kentaro Yasuchika[1], Takashi Nitta[1], Shinji Uemoto[1]

[1]*Department of Surgery, Graduate School of Medicine, Kyoto University, 54 Kawahara-cho, Shogoin, Sakyo-ku, Kyoto 606-8507, Japan;* [2]*Shiga Medical Center Research Institute, Moriyama, Moriyama-shi, Shiga 524-8524, Japan;* [3]*Department of Digestive Surgery, Mitsubishi Kyoto Hospital, Katsuragosho-cho, Nishikyo-ku, Kyoto 615-8087, Japan;* [4]*Department of Diagnostic Imaging and Nuclear Medicine, Graduate School of Medicine, Kyoto University, Kawahara-cho, Shogoin, Sakyo-ku, Kyoto 606-8507, Japan*

Background & Aims: This study investigated the relationship between tumor proliferative activity and the grade of tumor glucose metabolism or angiogenesis in hepatocellular carcinoma (HCC).

Methods: The study was performed as a retrospective analysis of 63 patients with HCC who underwent fluorine-18 fluorodeoxyglucose positron emission tomography (FDG-PET) as a preoperative examination prior to liver resection. Tumor proliferative activity was evaluated by the Ki-67 labeling index (LI). The grade of tumor glucose metabolism was evaluated by measuring the protein expression level of glucose transporter (GLUT)-1, expression level of pyruvate kinase type M2 (*PKM2*) mRNA, and FDG uptake. The grade of tumor angiogenesis was evaluated by the protein expression level of vascular endothelial growth factor (VEGF) and tumor microvessel density.

Results: All patients were divided into tertiles according to the Ki-67 LI: the low LI group ($n = 21$), the intermediate LI group ($n = 21$), and the high LI group ($n = 21$). The high LI group showed a tendency to have advanced tumor stage, and lower disease-free survival and overall survival rates than the low LI and the intermediate LI groups. The expression grade of GLUT-1, *PKM2* mRNA, and FDG uptake gradually increased with the Ki-67 LI. On the other hand, the protein expression grade of VEGF and microvessel density was paradoxically decreased with the Ki-67 LI.

Conclusions: These data suggest that (1) the proliferative activity of a resected specimen predicted the prognosis in patients with HCC; (2) the proliferative activity was closely correlated with the glucose metabolism, but not with angiogenesis.

© 2011 European Association for the Study of the Liver. Published by Elsevier B.V. All rights reserved.

Keywords: Fluorine-18 fluorodeoxyglucose positron emission tomography (FDG-PET); Vascular endothelial growth factor (VEGF); Micro vessel density; Glucose transporter-1 (GLUT-1); Pyruvate kinase type M2 (PKM2).
Received 15 September 2010; received in revised form 24 December 2010; accepted 10 January 2011; available online 18 February 2011

* Corresponding author. Tel.: +81 75 751 4323; fax: +81 75 751 4348.
E-mail address: etsu@kuhp.kyoto-u.ac.jp (E. Hatano).

Abbreviations: HCC, hepatocellular carcinoma; FDG-PET, ^{18}F-fluorodeoxyglucose positron emission tomography; SUV, standardized uptake value; TNR, tumor to non-tumor ratio of SUV; VEGF, vascular endothelial growth factor; MVD, microvessel density; GLUT-1, glucose transporter-1; PKM2, pyruvate kinase type M2; LI, labeling index; AFP, α-fetoprotein; DCP, des-gamma carboxy prothrombin; CRP, C-reactive protein; CT, computed tomography; MRI, magnetic resonance imaging; CI, confidence interval.

Introduction

Hepatocellular carcinoma (HCC) is one of the most common malignancies worldwide accounting for 500,000–600,000 deaths per year and the incidence will increase in future [1]. Hepatic resection and liver transplantation give the best outcome in well-selected candidates; however, the 5-year survival rate is still only 60–70% [2]. One of the reasons for the poor prognosis of HCC is the high rate of recurrence due to intrahepatic metastasis or the multicentric development of each neoplastic clone. Improving the survival rate of HCC requires that clinicians engage in active treatment of recurrence and explore and analyze biological or clinicopathological characteristics reflecting tumor behavior, such as progressive or metastatic capability.

Many biological or clinicopathological factors affecting the prognosis for patients with HCC have been investigated. Several clinical factors, such as tumor size, portal vein invasion, grade of cell differentiation, and the clinical stage of the tumor are important prognostic factors [3–5]. In addition, the prognosis of HCC patients is determined not only by clinical factors of the tumor *per se*, but also by other clinical factors, including the surgical procedure, the function, and histological features of the liver parenchyma bearing the HCC, and the presence of complications, such as esophageal varices [6,7]. Therefore, the present study focused on the prognosis of HCC patients who underwent hepatic resection before the performance of any other treatment in order to simplify the prognostic analysis. A histopathological analysis of the resected HCC specimen has an important prospective role in the management of patients who undergo liver resection. Therefore, this study retrospectively analyzed the biological characteristics of resected HCC specimens, including proliferative activity, glucose metabolism, and angiogenesis.

Author's personal copy

The proliferative activity of tumor cells is thought to be one of the most important prognostic factors in cancer patients. One of the most widely used proliferation-associated markers is Ki-67, which is a nuclear antigen present only in proliferating cells. The present study evaluated Ki-67 expression as a proliferative marker of the tumor itself, because Ki-67 immunostaining is easy-to-perform and can be commonly utilized as a cost-effective method for daily use in a clinical setting.

Recently, fluorine-18 fluorodeoxyglucose positron emission tomography (FDG-PET) has been utilized as oncologic diagnostic imaging, based on the enhanced glucose metabolism in cancer cells. FDG uptake is associated with prognosis in patients with HCC [8,9]. Glucose uptake in malignant tumors depends largely on the presence of the facilitated glucose transporter proteins and glycolytic enzymes. The glucose transporter isoform 1 (GLUT-1) is a key rate-limiting factor in the transport and metabolism of glucose in cancer cells and is overexpressed in a significant proportion of human carcinomas [10–12]. Pyruvate kinase (PK) regulates the rate-limiting final step of glycolysis, and the M2 isoform is upregulated in various malignant tumors [13,14]. The present study focused on these factors as parameters of glucose metabolism in addition to FDG uptake.

Tumor angiogenesis was also evaluated as a prognostic factor in HCC patients, because angiogenesis is essential for the growth and survival of solid tumors, and because anti-angiogenic therapy is an important option for the management of several human malignancies including HCC [15–17]. Studies in a variety of tumor types suggest that angiogenic molecular markers, such as vascular endothelial growth factor (VEGF) expression and intratumoral microvessel density are significant prognostic factors [18–20]. However, previous findings regarding the expression of VEGF in HCC are controversial. Some researchers reported that VEGF expression increases in advanced stage HCC [21,22], while others reported that VEGF plays an important role in the early phases of hepatocarcinogenesis rather than in advanced phases [23–25].

Some reports documented a correlation between proliferative activity and angiogenesis [26,27] and between proliferative activity and glucose metabolism in patients with HCC [28]. However, no report has evaluated glucose metabolism and angiogenesis together in comparison to proliferative activity in HCC. The aim

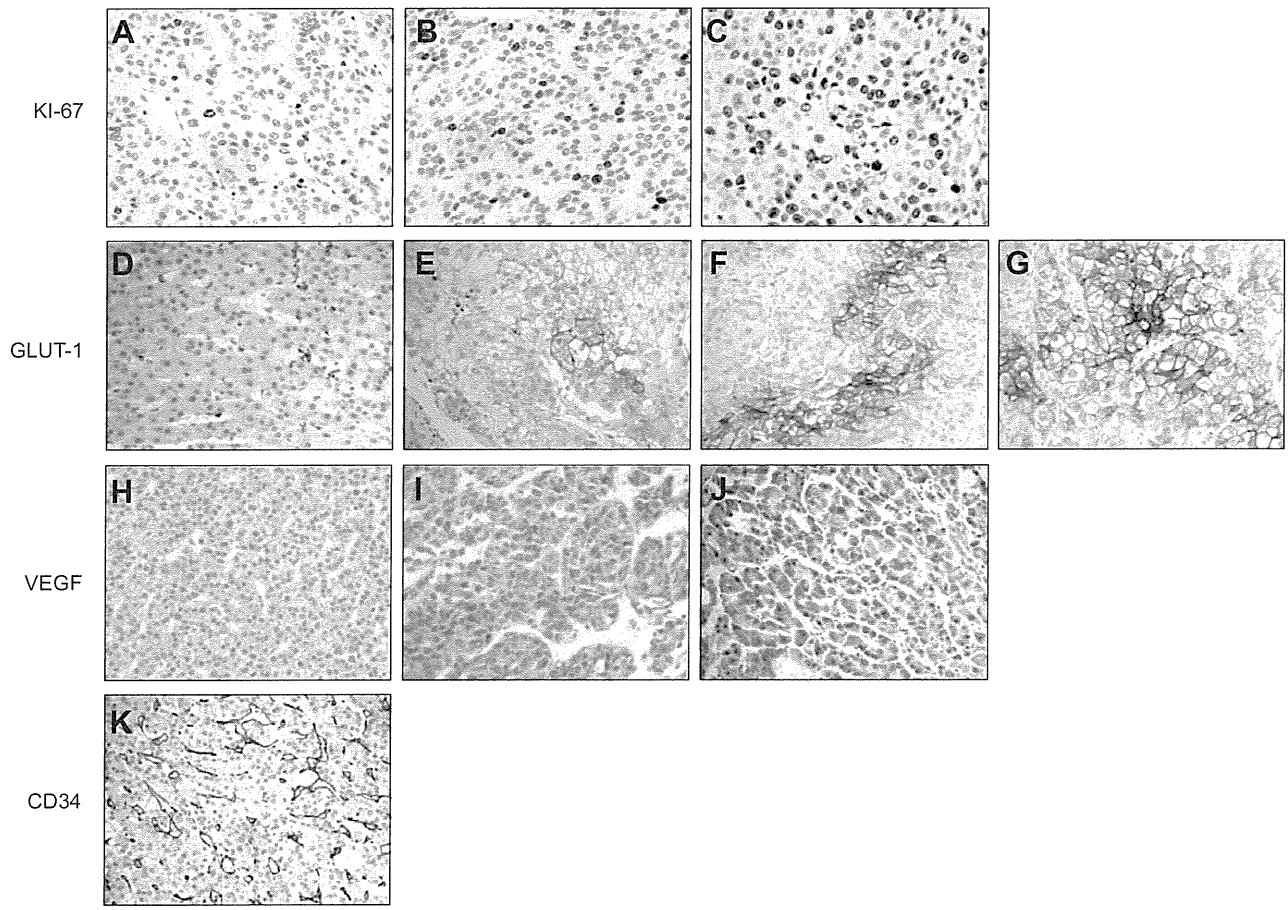

Fig. 1. Representative immunohistochemical figures of each score for Ki-67, GLUT-1, and VEGF staining, and representative figure for CD34 staining in tumoral tissue of HCC patients (original magnification, 200×). (A) Representative photomicrograph of the low Ki-67 labeling index (LI). (B) The intermediate Ki-67 LI. (C) The high Ki-67 LI. GLUT-1 expression was scored on a 5-point scale, (D) score 0, (E) score 1, (F) score 2, (G) score 3. VEGF expression scored on a 3-point scale (H) score 1 (I) score 2 (J) score 3. (K) Representative photomicrograph of CD34 expression.

Author's personal copy

of this study was to clarify the prognostic role of the proliferative activity of tumor cells and to evaluate how tumor proliferative activity is correlated with glucose metabolism and angiogenesis in patients with untreated HCC who underwent liver resection.

Patients and methods

Patients

The study was performed as a retrospective review of patients with HCC who underwent FDG-PET study as a preoperative examination and liver resection at the Department of Surgery, Kyoto University, between May 2003 and September 2005. Inclusion criteria in the present study were: (1) diagnosis of HCC by CT and magnetic resonance imaging, and pathologically confirmed, (2) patients who underwent hepatectomy within 2 weeks after the FDG-PET study. Exclusion criteria were: (1) patients who had distant metastasis, (2) patients who received pretreatment for HCC in the preoperative period. All patients were followed up with monthly monitoring of serum α-fetoprotein (AFP) and ultrasonography and/or contrast-enhanced CT every 3 months. Recurrence was confirmed by several imaging modalities, including CT and magnetic resonance imaging. Each patient provided written informed consent, as required by the Kyoto University Human Study Committee.

Immunohistochemistry

HCC samples were taken at the periphery of a tumor nodule to avoid necrotic areas and separated from adjacent nontumorous tissue. Paraffin sections were stained as previously described using the following antibodies: Ki-67 (#M7240, DAKO) diluted at 1:100, GLUT-1 (#A3536, DAKO) diluted at 1:200, VEGF (#sc-152, Santa Cruz Biotechnology, Santa Cruz, CA, USA) diluted at 1:200, and CD34 (#M7165, DAKO) diluted at 1:400 [9,29].

Paraffin sections were pretreated with 0.3% H_2O_2 in methanol for immunofluorescent chemistry of CD34 and GLUT-1, and then incubated in antigen-retriever solution containing citrate buffer (10 mM, pH 6.0) in a pressure cooker. The sections were incubated with blocking buffer for 1 h, the section were incubated with a primary antibody recognizing CD34 and GLUT-1 overnight at 4 °C. Subsequently, they were incubated with a 1:500 dilution of streptavidin Texas Red-X (#S6370, Invitrogen) conjugated goat anti-mouse IgG-B antibody (#sc2039, Santa Cruz), and then incubated with a 1:500 dilution of secondary Alexa Fluor 488 anti-rabbit IgG (#A21206, Invitrogen, CA, USA) each for 1 h at room temperature in the dark. The samples were then mounted with Vectashield (#H1000, VECTOR, CA, USA) with Hoechst (#H33342, Nacalai Tesque, Japan).

Quantification of the expression of Ki-67, GLUT-1, VEGF, and microvessel density in immunohistochemical staining

Ki-67 immunostaining was analyzed as a marker of proliferative activity. The number of positive stained nuclei of tumor cells was counted in at least 1000 tumor cells. The Ki-67 labeling index (LI) was classified in accordance with the percentage of positive tumor cells into tertiles; the Low LI group (L-LI; $n = 21$); the Intermediate LI group (I-LI; $n = 21$) and the High LI (H-LI; $n = 21$) (Fig. 1A–C).

The percentages of tumor cells with a strong immunoreactive membranous signal to GLUT-1 in the total number of tumor cells were counted in each of 10 low power fields (magnification 100×). The mean percentage of immunoreactive tumor cells was calculated and scored on a 5-point scale (0 = 0%, 1 = 1–25%, 2 = 26–50%, 3 = 51–75%, 4 = 76–100%) [12,30,31] (Fig. 1D–G).

The expression level of VEGF was determined by semiquantitative combined assessment of the percentage of stained tumor cells and the staining intensity [24,32–35]. The percentage of positive cells was counted and scored as: 1 point = 1–25% positive cells; 2 points = 26–50% positive cells; 3 points = 51–75% positive cells; and 4 points = 76–100% positive cells. The staining intensity was scored as: weak intensity: 1 point; moderate intensity: 2 points; and strong intensity: 3 points. Finally, both of these points were added, and specimens were scored from 1 to 3 according to their overall points: score 1 = total 2–3 points, score 2 = total 4–5 points, and score 3 = total 6–7 points (Fig. 1H–J).

Microvessel density in HCC was evaluated by the expression level of CD34 [36]. The positive stained area was evaluated using NIH image in 10 randomly chosen fields from each specimen. The percentage of CD34-positive area was calculated as the ratio to the pixel number of the whole area. A representative photomicrograph of CD34 is shown in Fig. 1K.

The evaluation of immunohistochemical staining for anti-Ki-67, anti-GLUT-1, and anti-VEGF antibodies was performed by three independent, experienced researchers who were blinded to any clinicopathological data, and the average score of three was adopted as the final score.

FDG-PET study

All PET imaging procedures were performed as described in our previous study [37].

Table 1. Patient characteristics of 63 patients with HCC.

Characteristic	Value
Age (years)	
Mean ± SD	65.6 ± 10.9
Range	32-80
Sex (male/female)	46/17
AFP	
<400 ng/ml	50
≥400 ng/ml	13
DCP	
<400 AU/ml	24
≥400 AU/ml	39
Etiology	
HBV	17
HCV	27
others	19
Child-Pugh classification	
A	59
B	4
Number of tumors	
Single	42
Multiple	21
Tumor size	
≤5 cm	31
>5 cm	32
Tumor differentiation	
Well	12
Moderately	33
Poorly	18
*Vascular invasion	
Absent	40
Present	23
†UICC T stage (T1/T2/T3/T4)	30/18/14/1
†UICC stage (I/II/III/IV)	30/17/16/0
SUV	
Mean ± SD	5.9 ± 4.7
Range	1.4-30.0
TNR (mean ± SD)	
Mean ± SD	2.2 ± 2.0
Range	0.6-13.3

AFP, α-fetoprotein; DCP, des-gamma carboxy prothrombin; SUV, standardized uptake value.
*Vascular invasion includes pathological portal vein invasion or hepatic vein invasion.
†TNM classification of the International Union Against Cancer (6th edition).

Author's personal copy

Image analysis

PET images were interpreted by at least two experienced nuclear medicine physicians, using all available clinical information and correlative conventional imaging for anatomic guidance. Regions of interest (ROIs) were manually defined on transaxial tomograms for semi-quantitative analysis of ^{18}F-FDG uptake. The ROI was drawn based on images from abdominal CT scans in patients that showed no significant high uptake by PET. The maximum standardized uptake value (SUV) was calculated for quantitative analysis of tumor ^{18}F-FDG uptake:

SUV = C(kBq/ml)/ID(kBq)/body weight(kg),

where C represents the tissue activity concentration measured by PET and ID represents the injected dose.

The tumor to non-tumor ratio (TNR) was also calculated:

TNR = Tumor SUV/Non-tumor SUV,

where the non-tumor SUV was defined as the average of SUVs at five points in non-tumor liver tissues.

Western blot analysis

Western blot analysis was performed as described previously [29] with a primary antibody against GLUT-1 at 1:1000 dilution in Blocking-One, an anti-VEGF antibody at 1:400 dilution, and an anti-actin antibody (#sc-1615; Santa Cruz Biotechnology, Santa Cru, CA, USA) at 1:1000 dilution. The intensity of the bands was quantified with Quantity One imaging analysis software (Bio-Rad Laboratories, Hercules, CA, USA) and normalized with actin as an internal control.

Quantitation of PKM2 mRNA by Real-time reverse transcription polymerase chain reaction (RT-PCR) assay

Total RNA was extracted from frozen tumorous liver tissues using the TRIzol reagent (Invitrogen Japan, Tokyo, Japan). Total RNA (2 μg) was reverse transcribed to cDNA with an Omniscript RT Kit (Qiagen in Japan, Tokyo, Japan) with oligo (dT) primers (Invitrogen Japan). Real-time RT-PCR was performed with a SYBR Green I master (Roche Diagnostics GmbH, Mannheim, Germany) and LightCycler 480 (Roche Diagnostics GmbH). *PKM2* primers were as follows, forward primer:

Table 2. Comparison of clinicopathological factors in three groups according to the Ki-67 labeling index.

Factor	Variable	Ki-67 LI			*p* value
		L-LI group (n = 21)	I-LI group (n = 21)	H-LI group (n = 21)	
Age	<65	6	8	13	0.080
	≥65	15	13	8	
Sex	male	19	14	15	0.159
	female	2	7	6	
AFP (ng/ml)	≤400	21	16	13	0.009
	>400	0	5	8	
DCP (AU/ml)	≤400	11	5	8	0.162
	>400	10	16	13	
Etiology	HBV	4	4	9	0.097
	HCV	13	9	5	
	others	4	8	7	
Child-Pugh	A	20	19	20	0.766
	B	1	2	1	
Number of tumors	single	15	18	9	0.011
	multiple	6	3	12	
Tumor size	≤5cm	12	11	8	0.438
	>5cm	9	10	13	
Tumor differentiation	well	9	4	0	<0.001
	mod	12	14	7	
	poor	0	3	14	
*Vascular invasion	absent	19	15	6	<0.001
	present	2	6	15	
†UICC T stage	T1	13	13	4	0.006
	T2-T4	8	8	17	
†UICC stage	I	13	13	4	0.006
	II, III	8	8	17	

L-LI group, low labeling index group; I-LI group, intermediate labeling group; H-LI group, high labeling index group; AFP, α-fetoprotein; DCP, des-gamma carboxy prothrombin; well, well differentiated; mod, moderately differentiated; poor, poorly differentiated.
*Vascular invasion includes pathological portal vein invasion or hepatic vein invasion.
†TNM classification of the International Union Against Cancer (6th edition).

Author's personal copy

5′-GAGTACCATGCGGAGACCAT-3′; reverse primer: 5′-GCGTTATCCAGCGTGATTTT-3′. As an internal control, we amplified human *β-actin* with the following primer set, forward primer: 5′-GCGGGAAATCGTGCGTGACAT-3′; reverse primer: 5′-GATGGAGTTGAAGGTAGTTTGTG-3′. RT-PCR was performed with an initial step at 95 °C for 15 min, followed by 40 cycles at 95 °C for 30 s, 56 °C for 30 s, and 72 °C for 1 min with a final step at 72 °C for 10 min. The expression levels were calculated after conversion to numerical values by LightCycler 480 software and are shown as ratios relative to the expression level of β-actin.

Statistical analysis

Statistical analysis was performed using the SPSS v. 11.0.1 software package (SPSS Inc., Chicago, IL, USA). All values are expressed as the means ± standard error of the mean (SEM). Correlations between clinicopathological parameters between each group were assessed using χ^2 test. The statistical significance of a difference between each group was assessed using nonparametric statistical tests (Mann–Whitney *U*-test). Survival time was defined from the date of surgery until the date of death, and the end point for disease-free survival was defined as the date when recurrence was detected by various modalities, such as CT, MRI, and FDG-PET. The cumulative disease-free survival rate and cumulative overall survival rate were analyzed using the Kaplan–Meier methods, and differences in survival between the groups were compared using a log-rank test. A p value <0.05 was considered to be statistically significant.

Results

Patient characteristics

One hundred and twenty-six patients with HCCs underwent liver resection between May 2003 and September 2005 at Kyoto University Hospital. Thirteen of these patients did not undergo preoperative FDG-PET and 52 received previous treatment for HCC including liver resection ($n = 16$), transarterial chemoembolization (TACE, $n = 42$) or percutaneous ethanol injection therapy (PEIT, $n = 4$), and the remaining 63 patients were enrolled in this study. The clinical characteristics of the 63 patients are shown in Table 1.

Relationship between Ki-67LI and clinicopathological parameters

The mean percentage of Ki-67 positive cells was 16.9% (range: 0.0–64.4). The 63 patients were divided into tertiles; the L-LI group ($n = 21$; 0.0–3.9), the I-LI group ($n = 21$; 4.5–17.8), and the H-LI group ($n = 21$; 19.1–64.4). The relationship between Ki-67 LI and the clinicopathological parameters in these patients is shown in Table 2. The H-LI group showed a tendency to have higher serum AFP levels, multiple tumors, poorly differentiated tumors, presence of vascular invasion, advanced T stage, and advanced tumor stage, in comparison to the L-LI and the I-LI groups.

Disease free rates and survival rates according to Ki-67 labeling index

The mean follow-up periods in 63 patients was 38 months (range, 2.5–66.7 months), and postoperative recurrence developed in 47 (74.6%) patients, including 35 patients with intrahepatic recurrence, 8 patients with lung metastases, 1 patient each with bone metastasis, gland metastasis, and lymph node metastases. The median disease-free time and overall survival time in 63 patients were 17.7 months and 51.9 months, respectively. The disease-free rate and survival rate in each group are shown in Fig. 2A and B. The cumulative disease free survival rate of the H-LI group was significantly lower in comparison to those of both the I-LI group ($p < 0.05$) and the L-LI group ($p < 0.01$). Similarly, the patients in the H-LI group had the worst median survival, in comparison to those in both the I-LI group and the L-LI group (the H-LI group; 23.0 months, the I-LI group; 45.6 months, and the L-LI group; 56.9 months, $p < 0.01$). The five-year survival rate in each group was 33.3%, 45.7%, and 69.8% in the H-LI group, I-LI group, and L-LI group, respectively.

Relationship of GLUT-1 and PKM2 expression with SUV and TNR

The 63 patients were classified into two groups based on the SUV: the high SUV group (SUV ⩾5) and low SUV group (SUV

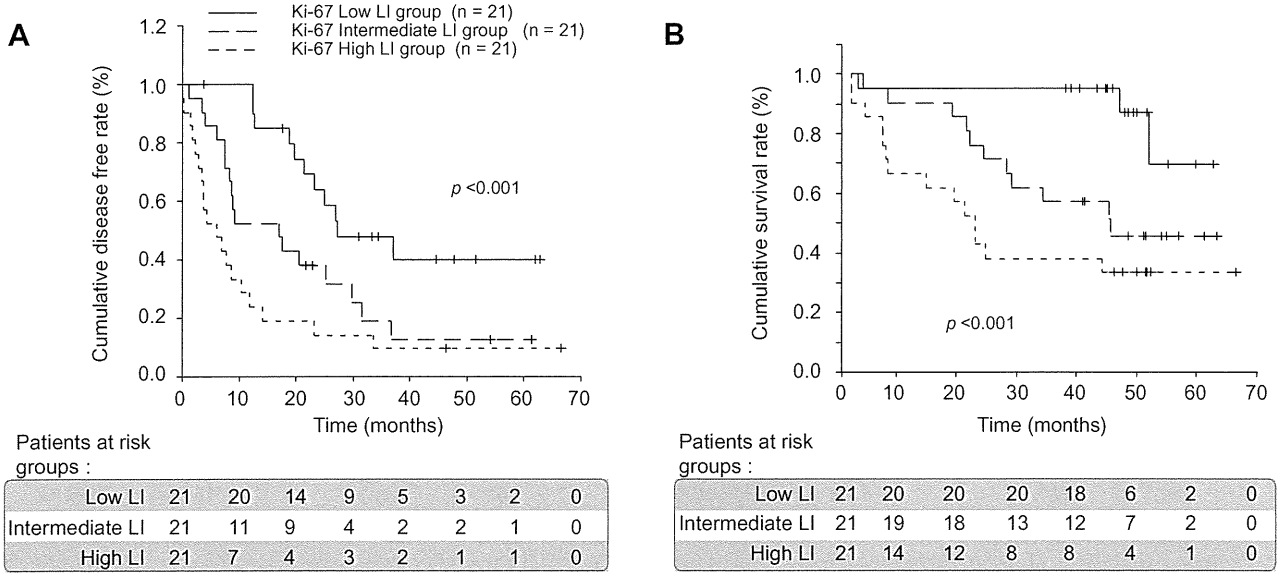

Fig. 2. Cumulative disease free and overall survival rates of HCC patients analyzed by Kaplan–Meier analysis and log-rank test. (A) The cumulative disease free rate of HCC patients with the three groups of Ki-67 LI. (B) The cumulative survival rate of HCC patients with the three groups. LI, labeling index.

Author's personal copy

<5), or TNR: high TNR group (TNR ⩾2) and low TNR group (TNR <2) [8,9]. Immunohistochemical staining showed that GLUT-1 expression was positively correlated with SUV (r = 0.758; Fig. 3A) and TNR (r = 0.715; Fig 3B. There was no case that scored point 4 for GLUT-1 expression). The mean value of GLUT-1 expression in the high SUV group (n = 28; 1.2 ± 0.2) was significantly higher than that of the low SUV group (n = 35; 0.1 ± 0.1; p <0.01, Fig. 3C), and with the number of patients with high TNR (n = 19; 1.4 ± 0.3) was significantly higher than that of the low TNR group (n = 44; 0.2 ± 0.1; p <0.01; Fig. 3D). *PKM2* mRNA expression was weakly correlated with SUV (r = 0.528; Fig. 3E) and TNR (r = 0.343; Fig. 3F), respectively. The mean value of *PKM2* mRNA with high SUV group (n = 22; 2.0 ± 0.3) was significantly higher than that of the low SUV group (n = 24; 0.8 ± 0.1; p <0.01, Fig. 3G); and that of the high TNR group (n = 14; 2.5 ± 0.5) was significantly higher than that of the low TNR group (n = 32; 0.9 ± 0.1; p <0.01, Fig. 3H). These results indicate that FDG uptakes reflect increased glucose transport and glycolysis.

Relationship of Ki-67 LI with glucose metabolism; GLUT-1, PKM2, SUV, and TNR

A comparison of the absolute values revealed a positive correlation between Ki-67 LI and GLUT-1 (r = 0.838; Supplementary Fig. 1A), PKM2 (r = 0.386; Supplementary Fig. 1B), SUV (r = 0.679; Supplementary Fig. 1C), TNR (r = 0.707; Supplementary Fig. 1D), respectively. The mean value of GLUT-1 expression quantified by immunohistochemical staining in the H-LI group (1.4 ± 0.2) was significantly higher than that in the I-LI group (0.2 ± 0.1; p <0.01) and that in the L-LI group (0.0 ± 0.0; p <0.01;

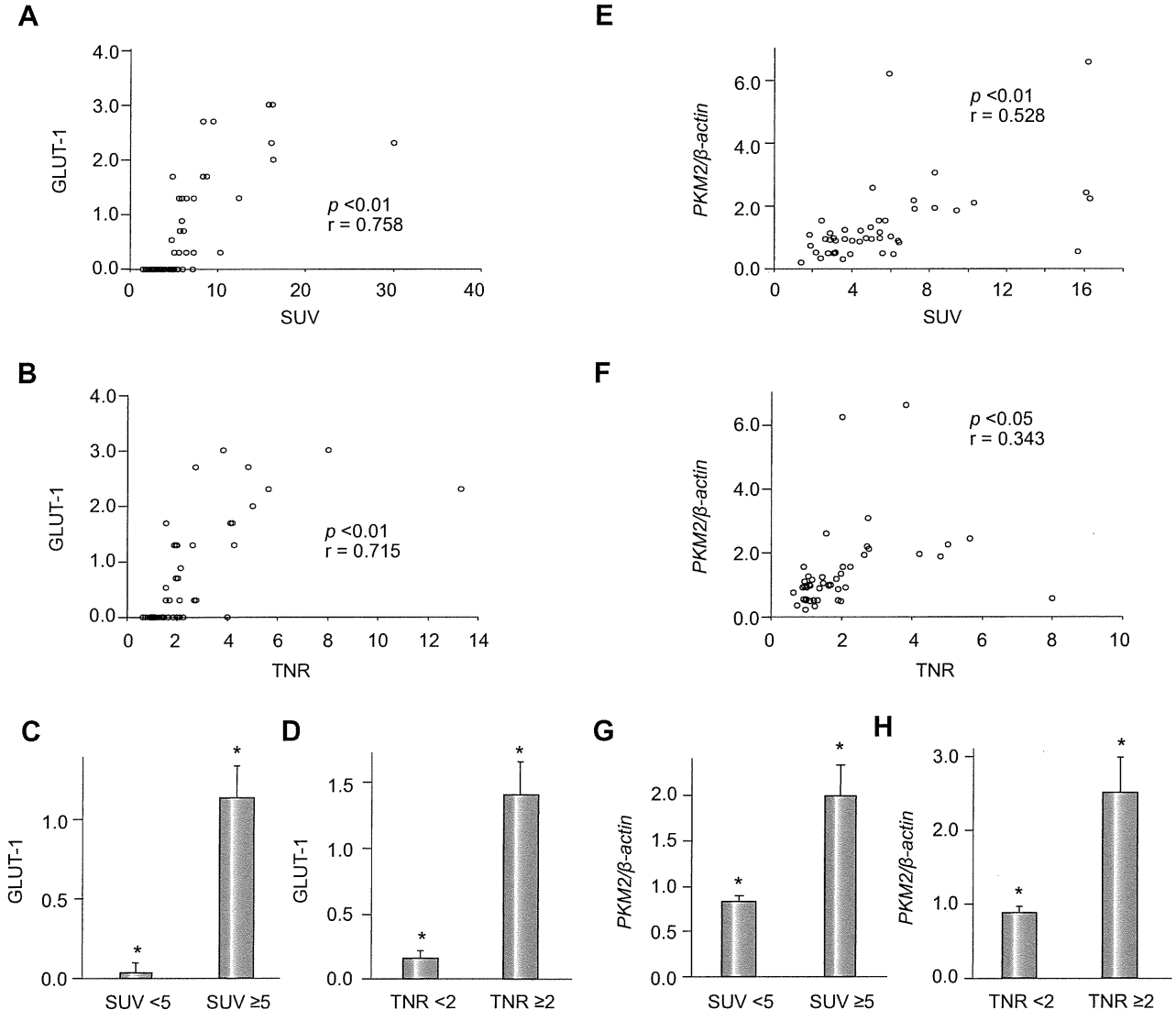

Fig. 3. Relationship of GLUT-1 and *PKM2* mRNA expressions with SUV and TNR. (A) Relationship between GLUT-1 quantified by immunohistochemical staining and SUV in HCC. (B) Relationship between GLUT-1 quantified by immunohistochemical staining and TNR. (C) The mean value of GLUT-1 expression with SUV <5 group (n = 35) and SUV ⩾5 group (n = 28). (D) The mean value of GLUT-1 expression with TNR <2 group (n = 44) and TNR ⩾2 group (n = 19). (E) Relationship between *PKM2* quantified by real-time RT-PCR and SUV. (F) Relationship between *PKM2* quantified by real-time RT-PCR and TNR in HCC. (G) The mean value of *PKM2* mRNA with SUV <5 group (n = 24) and SUV ⩾5 group (n = 22). (H) The mean value of *PKM2* mRNA with TNR <2 group (n = 32) and TNR ⩾2 group (n = 14). Data are shown as the means ± SEM. *p <0.01.

Author's personal copy

Fig. 4A). Western blot analysis of GLUT-1 protein was performed on 46 tumor tissue sections of 46 patients with HCC, and normal liver tissues were obtained from 6 patients and also analyzed as a control. Western blotting showed that the mean value of GLUT-1 expression in the H-LI group ($n = 16$; 0.5 ± 0.1) was significantly higher than that in the I-LI group ($n = 14$; 0.2 ± 0.1; $p < 0.05$) and that in the L-LI group ($n = 16$; 0.2 ± 0.1; $p < 0.05$; Fig. 4B and C). The mean value of *PKM2* mRNA expression in the H-LI group ($n = 16$; 2.1 ± 0.5) was significantly higher than that in the L-LI group ($n = 16$; 0.8 ± 0.1; $p < 0.05$), and was not significantly higher than that in the I-LI group ($n = 14$; 1.2 ± 0.2; $p = 0.26$; Fig. 4D). The SUV in the H-LI group (9.0 ± 1.4) was significantly higher than that in the I-LI group (5.4 ± 0.7; $p < 0.01$); and that in the I-LI group was significantly higher than that in the L-LI group (3.3 ± 0.3; $p < 0.01$; Fig. 4E). TNR in the H-LI group (3.4 ± 0.6) was significantly higher than that in the I-LI group (1.8 ± 0.2; $p < 0.01$); and that in the I-LI group was significantly higher than that in the L-LI group (1.2 ± 0.1; $p < 0.01$; Fig. 4F). These results suggest that tumor glucose metabolism in HCC is gradually increased in association with the Ki-67 LI.

Relationship of Ki-67 LI with tumor angiogenesis, VEGF, and microvessel density

A comparison of the absolute values revealed a negative correlation between Ki-67 LI and VEGF ($r = -0.651$; Supplementary Fig. 1E), microvessel density ($r = -0.604$; Supplementary Fig. 1F), respectively. The mean value of VEGF expression in the H-LI group (1.3 ± 0.1) was significantly lower than that in the I-LI group (2.0 ± 0.1; $p < 0.01$); and that in the I-LI group was significantly lower than that in the L-LI group (2.4 ± 0.1; $p < 0.05$; Fig. 5A). The mean value of microvessel density in the H-LI group (4.0 ± 0.8) was significantly lower than that in the I-LI group (9.2 ± 0.9; $p < 0.01$), and that in the I-LI group was significantly

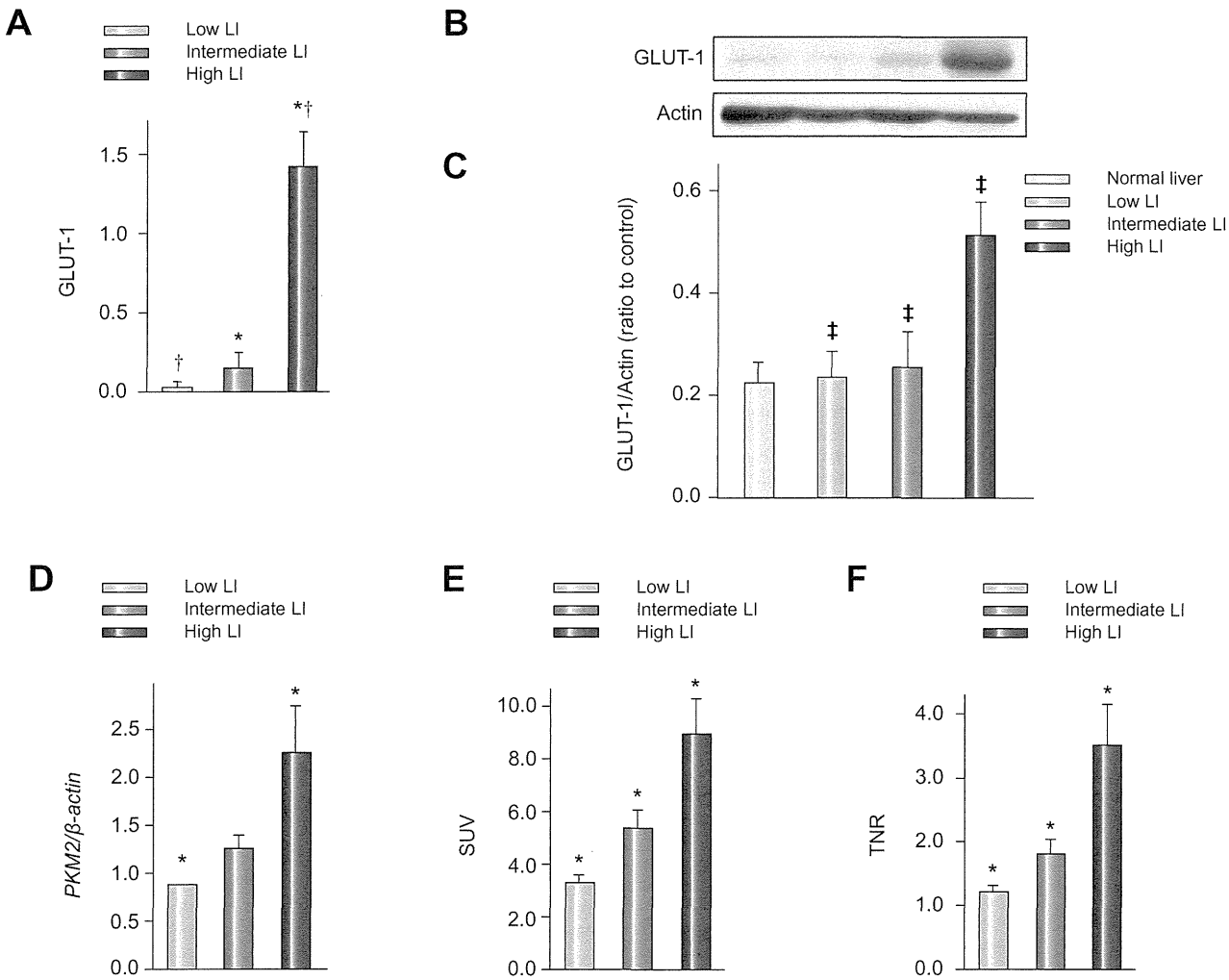

Fig. 4. Relationship of Ki-67 LI with glucose metabolism; GLUT-1, *PKM2*, SUV, and TNR. (A) The mean value of GLUT-1 expression quantified by immunohistochemical staining with the three groups of Ki-67 LI. (B) A Western blot analysis of GLUT-1 was performed among the four groups and (C) the Western blot was analyzed densitometrically. (D) Quantitative real-time RT-PCR of pyruvate kinase *PKM2* with the three groups of Ki-67 LI. (E) The mean value of standardized uptake value (SUV) with the three groups of Ki-67 LI. (F) The mean value of tumor to non-tumor ratio of SUV (TNR) with the three groups of Ki-67 LI. Data are shown as means ± SEM. *$p < 0.01$, †$p < 0.01$, ‡$p < 0.05$. L, low; I, intermediate; H, high; LI, labeling index; NL, normal liver.

Author's personal copy

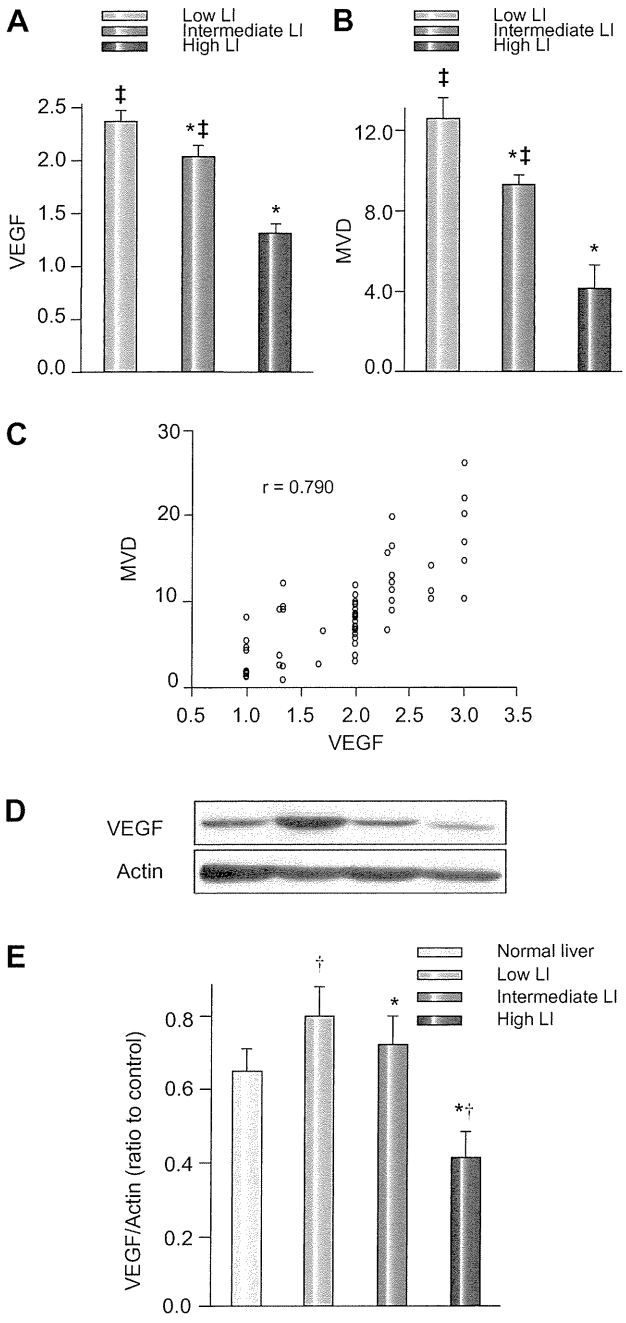

Fig. 5. Relationship of Ki-67 LI with tumor angiogenesis in HCC. (A) The mean value of VEGF expression quantified by immunohistochemical staining with the three groups of Ki-67 LI. (B) The mean value of MVD (analyzed by immunohistochemical staining of CD34 expression) with the three groups of Ki-67 LI. (C) Relationship between VEGF expression and MVD in HCC. (D) A Western blot analysis of VEGF was performed among the four groups and (E) the Western blot was analyzed densitometrically. Data are shown as means ± SEM. $^{*}p$ <0.01, $^{\dagger}p$ <0.01, $^{\ddagger}p$ <0.05. L, low; I, intermediate; H, high; LI, labeling index; MVD, microvessel density; NL, normal liver.

lower than that in the L-LI group (12.6 ± 1.2; p <0.05; Fig. 5B). VEGF expression was positively correlated with the microvessel density (r = 0.790; Fig 5C). Western blotting showed that the mean value of VEGF expression in H-LI group (n = 16; 0.4 ± 0.0) was significantly lower than that of the I-LI group (n = 14; 0.7 ± 0.1; p <0.01) and the L-LI group (n = 16; 0.8 ± 0.1; p <0.01; Fig. 5D and E). This correlation between Ki-67 LI and VEGF was comparable to that observed by immunohistochemistry. These results suggest that tumor angiogenesis in HCC is gradually decreased in comparison to the Ki-67 LI.

Disease free rates and survival rates according to GLUT-1, VEGF, and microvessel density

Using the median values of immunostaining as cutoffs, patients were classified into high GLUT-1 (>0) and low GLUT-1 (⩽0) groups, high VEGF (⩾2.0) and low VEGF (<2.0) groups, and high microvessel density (⩾8.4) and low microvessel density (<8.4) groups. The cumulative disease free survival rate of the high GLUT-1 group was significantly lower compared with the low GLUT-1 group (p <0.001; Fig. 6A), and the low microvessel density group was also significantly lower compared with the high microvessel density group (p = 0.021; Fig 6C). The survival rate of the high GLUT-1 group was significantly lower compared with the low GLUT-1 group (p <0.001; Fig. 6D), the low VEGF group was significantly lower compared with the high VEGF group (p = 0.041; Fig. 6E), and the low microvessel density group was also significantly lower compared with the high microvessel density group (p = 0.049; Fig. 6F).

Localization of GLUT-1 expression in HCC

Immunofluorescence examination of GLUT-1 and CD34 showed no correlation between the localization of GLUT-1 and CD34 expression in hepatocellular carcinoma tissue. GLUT-1 expression was predominantly observed in a ring-shaped area, which was localized in a circular pattern surrounding CD34 positive tumor vessels from a distance of at least 100 μm (Fig. 7). These results indicate that GLUT-1 was mainly expressed in a relatively-hypoxic area away from the tumor vessels.

Discussion

Many factors including the condition of the liver, tumor factors, surgical procedures, and the presence/absence of postoperative complications affect the prognosis in patients with HCC. In this study, Ki-67 and other markers were compared and evaluated to determine the relationship between proliferative activity in the tumor, recurrence and prognosis, and other tumor factors. Patients were assigned to three groups based on tumor proliferative activity, to classify the risk of postoperative recurrence, prognosis, and treatment strategy. In breast cancers, proliferative rate assessed from Ki-67 staining is routinely used as a prognostic marker to modify therapeutic choice and to predict benefit from adjuvant therapy [38–40]. Adjuvant therapy and careful follow-up are required for the high-risk of recurrence in HCC patients. The current series demonstrated that the expression of Ki-67 was considerably correlated with the cumulative disease free survival rate. From these findings, we expect that Ki-67 of resected HCC specimens could be helpful for defining the indication of adjuvant therapy. It is important to select the appropriate patient population for a randomized study of postoperative adjuvant therapy [41].

Author's personal copy

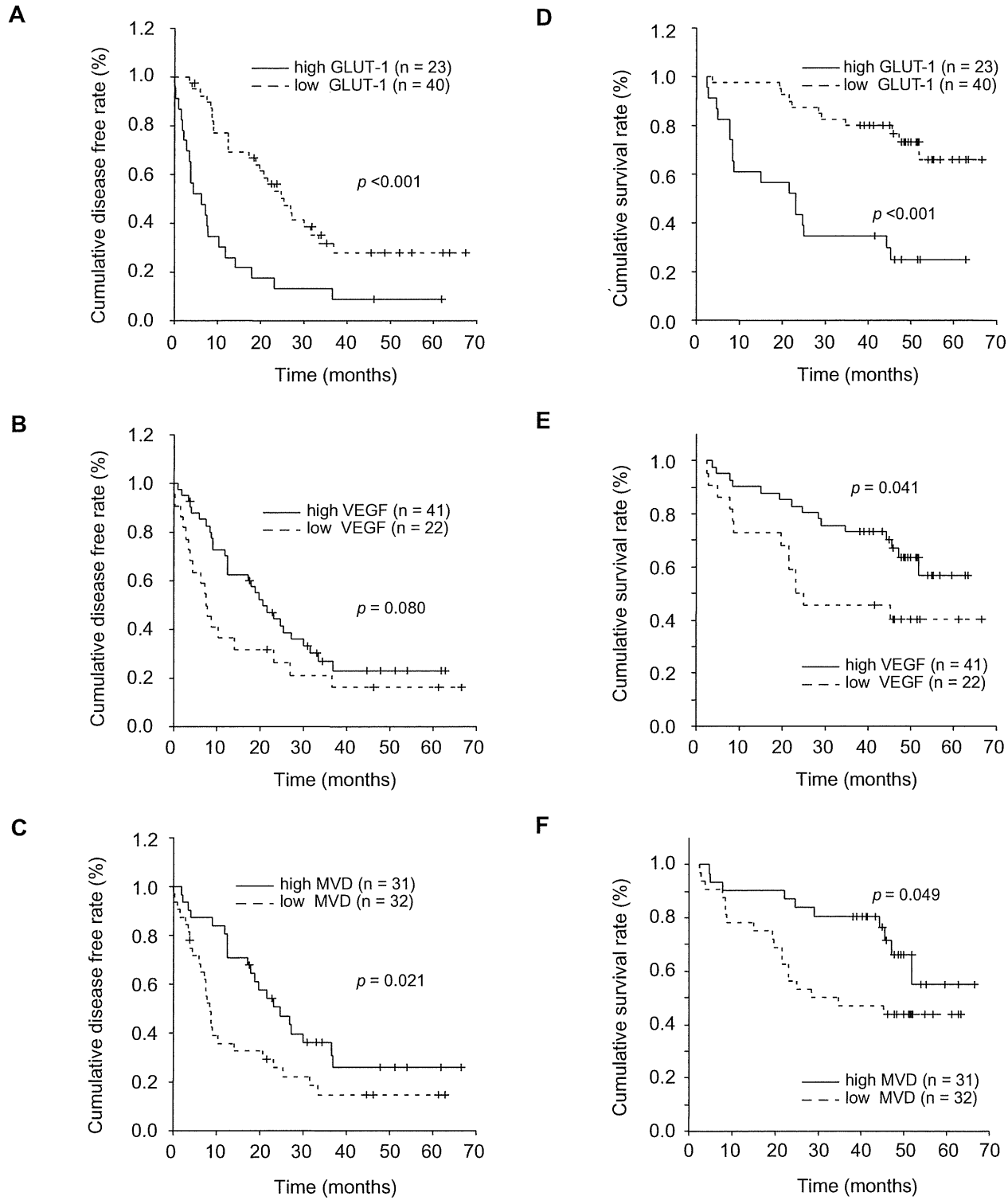

Fig. 6. Cumulative disease free and overall survival rates of HCC patients analyzed by Kaplan–Meier analysis and log-rank test. (A–C) The cumulative disease free rates of HCC patients with the two groups of GLUT-1, VEGF, and microvessel density. (D–F) The cumulative survival rates of HCC patients with the two groups of GLUT-1, VEGF, and microvessel density. MVD, microvessel density.

Glucose uptake in malignant tumors depends largely on the presence of the facilitated glucose transporter proteins. GLUT-1 is the major GLUT in a variety of tumor cells, such as non-small cell lung carcinoma, colorectal carcinoma, and gastric carcinoma.

Author's personal copy

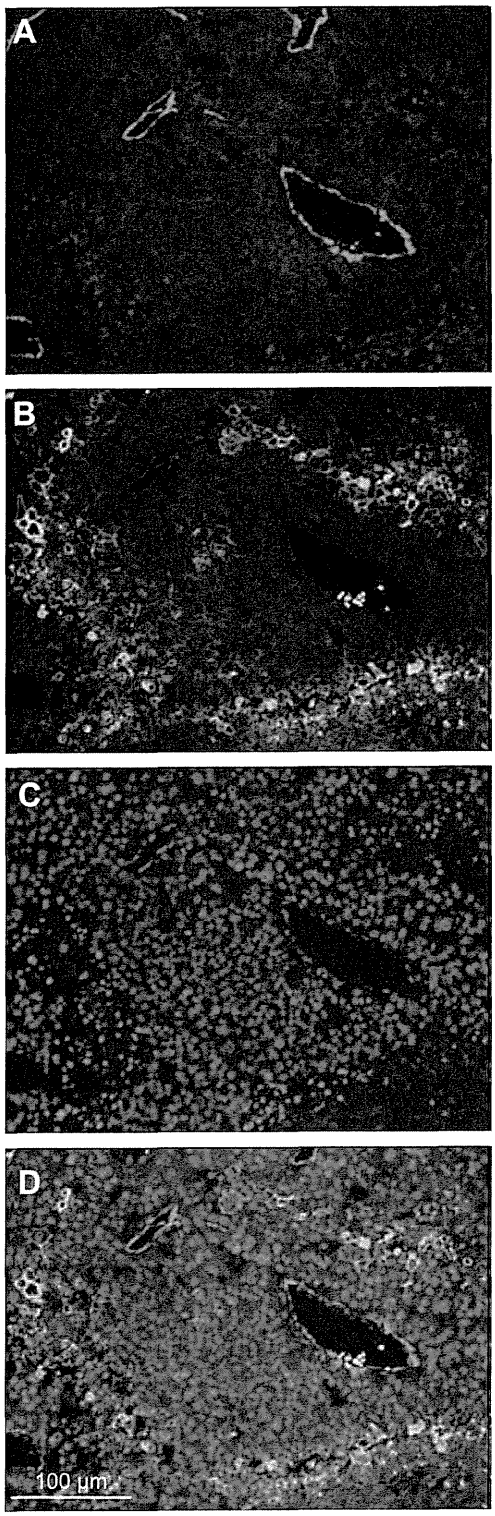

Fig. 7. Immunofluorescence for CD34 (A, red), GLUT-1 (B, green), and counterstained by Hoechst (C, blue) in the tumoral tissue of an HCC patient. The merge image (D) shows the localization of GLUT-1 and microvessels in HCC. (For interpretation of the references to colour in this figure legend, the reader is referred to the web version of this article.)

However, GLUT-1 is not well expressed in the normal liver and HCC, because the liver mainly expresses a different glucose transporter protein known as GLUT-2 [42]. The expression of GLUT-1 is detected in less than 10% of human HCC tissues, but is increased under hypoxic conditions in HCC cell lines [28]. Animal studies have shown the expression of GLUT-1 especially around the terminal hepatic vein [43]. The current study demonstrated that GLUT-1 was overexpressed in the high Ki-67 group, in which the mean value of angiogenesis was low, and its expression was predominantly observed in the area far from the tumor vessels. These findings suggest that GLUT-1 is upregulated in HCC with high proliferative activity, and overexpressed especially in hypoxic regions.

Pyruvate kinase (PK), a rate-limiting enzyme during glycolysis, catalyzes the production of pyruvate and adenosine 5′-triphosphate (ATP) from phosphoenolpyruvate (PEP) and adenosine 5′-diphosphate (ADP). PKM2 is found predominantly in the fetus and also in cancer cells, where the abundance of other isoforms of PK is low. Recently, Christofk *et al.* found that PKM2 is necessary for aerobic glycolysis and cell proliferation *in vivo* [44,45]. Other biochemical studies found that both the activity and amount of PKM2 increased in hepatocellular tumors [46,47]. In the current study, we observed that *PKM2* mRNA expression was related to FDG uptake, and the high Ki-67 LI group tended to show higher *PKM2* mRNA expression and FDG uptake than low or intermediate LI groups. These results indicate that regulation of glycolysis via GLUT-1 and PKM2 may influence the proliferative activity of HCC to a certain extent.

Angiogenesis is essential for the growth and survival of solid tumors. Studies in a variety of tumor types suggest that angiogenic molecular markers, such as VEGF and intratumoral microvessel density are significant prognostic factors [18–20]. However, the relationship between angiogenesis and prognosis is somewhat different in HCC. VEGF has been reported to play an important role in the early phases of hepatocarcinogenesis rather than in advanced phases [23]. It was also reported that VEGF expression is frequently detected in well-differentiated HCC rather than in moderately to poorly differentiated HCC [24,25,48]. Sarcomatous HCCs are categorized as undifferentiated tumors with the strongest malignant potential in HCC. Others reported a case study of sarcomatous HCC in which VEGF expression was not abundant [25,49,50]. These findings support the present results, angiogenesis estimated by VEGF and microvessel density decreased in Ki-67 LI, and lead us to suggest that the increase of angiogenetic factors may not be directly associated with proliferative activity, i.e., prognosis in HCC.

The present study analyzed the glucose metabolism by assessing the expression of GLUT-1 protein, *PKM2* mRNA, and FDG uptake in HCC, and showed that all three increased in Ki-67 LI, whereas the angiogenesis evaluated by VEGF and the microvessel density paradoxically decreased. These results lead to the assumption that there was an inverse correlation between tumor glucose metabolism and angiogenesis in HCC. In tumor progression, hypoxia is an important condition in various pathological processes. Induction of hypoxia-inducible factor (HIF) results in the up-regulation of a variety of target genes including genes involved in cell proliferation, glucose metabolism, and angiogenesis [51]. On the other hand, a recent report demonstrated that accelerated perinecrotic outgrowth of liver tumor following radiofrequency ablation was a hypoxia-driven phenomenon controlled by the HIF pathway, in which VEGF was not involved [52]. This report indicated that

Author's personal copy

hypoxia does not always up-regulate VEGF. In the clinical setting, tumors, which survive and grow despite deprivation of the blood supply by TAE, sometimes show aggressive phenotype and become resistant to repeated TAE. These observations may be explained by the metabolic alternation; a complementary pattern of glucose metabolism and tumor angiogenesis in tumors. Further studies would be needed to clarify the correlation between hypoxia, glucose metabolism, and angiogenesis in HCC.

Several angiogenesis inhibitors, such as bevacizumab, have been developed and are routinely used in clinical practices [15,16]. However, there is no appropriate diagnostic imaging modality that can evaluate angiogenesis specifically *in vivo*. FDG-PET is the only diagnostic imaging modality that can evaluate metabolic change in cancer after these kinds of molecular targeting therapies [53,54]. However, the current data suggest that it might be difficult to accurately evaluate angiogenesis in patients with HCC by FDG-PET. There is an urgent need to develop novel *in vivo* markers to assess molecular targeting angiogenic therapies. On the other hand, there is a possibility that angiogenesis inhibitors may induce hypoxia in tumor tissues and then stimulate increased glucose metabolism with higher proliferative activity in HCC. In these cases, FDG-PET may have a prognostic role in the evaluation of transformed HCCs after these molecular targeting angiogenic therapies. In addition, more recent studies have provided supporting evidence that inhibition of glycolysis may exert preferential effect on cancer cells [55]. FDG-PET might be a good surrogate marker in determining the indication of those therapies.

In conclusion, the present data suggest that proliferative activity of resected specimen showed a significant prognostic role in patients with HCC. It was also suggested that proliferative activity showed a close correlation with glucose metabolism, but not with angiogenesis.

Conflict of interest

The authors who have taken part in this study declared that they do not have anything to disclose regarding funding or conflict of interest with respect to this manuscript.

Supplementary data

Supplementary data associated with this article can be found, in the online version, at doi:10.1016/j.jhep.2011.01.038.

References

[1] Ince N, Wands JR. The increasing incidence of hepatocellular carcinoma. N Engl J Med 1999;340:798–799.

[2] Llovet JM, Burroughs A, Bruix J. Hepatocellular carcinoma. Lancet 2003;362: 1907–1917.

[3] Predictive factors for long term prognosis after partial hepatectomy for patients with hepatocellular carcinoma in Japan. The Liver Cancer Study Group of Japan. Cancer 1994;74:2772–2780.

[4] Izumi R, Shimizu K, Ii T, Yagi M, Matsui O, Nonomura A, et al. Prognostic factors of hepatocellular carcinoma in patients undergoing hepatic resection. Gastroenterology 1994;106:720–727.

[5] Nonami T, Harada A, Kurokawa T, Nakao A, Takagi H. Hepatic resection for hepatocellular carcinoma. Am J Surg 1997;173:288–291.

[6] Ikeda K, Saitoh S, Koida I, Arase Y, Tsubota A, Chayama K, et al. A multivariate analysis of risk factors for hepatocellular carcinogenesis: a prospective observation of 795 patients with viral and alcoholic cirrhosis. Hepatology 1993;18:47–53.

[7] Nagasue N, Uchida M, Makino Y, Takemoto Y, Yamanoi A, Hayashi T, et al. Incidence and factors associated with intrahepatic recurrence following resection of hepatocellular carcinoma. Gastroenterology 1993;105:488–494.

[8] Hatano E, Ikai I, Higashi T, Teramukai S, Torizuka T, Saga T, et al. Preoperative positron emission tomography with fluorine-18-fluorodeoxyglucose is predictive of prognosis in patients with hepatocellular carcinoma after resection. World J Surg 2006;30:1736–1741.

[9] Seo S, Hatano E, Higashi T, Hara T, Tada M, Tamaki N, et al. Fluorine-18 fluorodeoxyglucose positron emission tomography predicts tumor differentiation, P-glycoprotein expression, and outcome after resection in hepatocellular carcinoma. Clin Cancer Res 2007;13:427–433.

[10] Medina RA, Owen GI. Glucose transporters: expression, regulation and cancer. Biol Res 2002;35:9–26.

[11] Higashi T, Tamaki N, Torizuka T, Nakamoto Y, Sakahara H, Kimura T, et al. FDG uptake, GLUT-1 glucose transporter and cellularity in human pancreatic tumors. J Nucl Med 1998;39:1727–1735.

[12] Higashi T, Saga T, Nakamoto Y, Ishimori T, Mamede MH, Wada M, et al. Relationship between retention index in dual-phase (18)F-FDG PET, and hexokinase-II and glucose transporter-1 expression in pancreatic cancer. J Nucl Med 2002;43:173–180.

[13] Spoden GA, Rostek U, Lechner S, Mitterberger M, Mazurek S, Zwerschke W. Pyruvate kinase isoenzyme M2 is a glycolytic sensor differentially regulating cell proliferation, cell size and apoptotic cell death dependent on glucose supply. Exp Cell Res 2009;315:2765–2774.

[14] Mazurek S, Boschek CB, Hugo F, Eigenbrodt E. Pyruvate kinase type M2 and its role in tumor growth and spreading. Semin Cancer Biol 2005;15: 300–308.

[15] Hurwitz H, Fehrenbacher L, Novotny W, Cartwright T, Hainsworth J, Heim W, et al. Bevacizumab plus irinotecan, fluorouracil, and leucovorin for metastatic colorectal cancer. N Engl J Med 2004;350:2335–2342.

[16] Johnson DH, Fehrenbacher L, Novotny WF, Herbst RS, Nemunaitis JJ, Jablons DM, et al. Randomized phase II trial comparing bevacizumab plus carboplatin and paclitaxel with carboplatin and paclitaxel alone in previously untreated locally advanced or metastatic non-small-cell lung cancer. J Clin Oncol 2004;22:2184–2191.

[17] Folkman J. Angiogenesis: an organizing principle for drug discovery? Nat Rev Drug Discov 2007;6:273–286.

[18] Kleespies A, Guba M, Jauch KW, Bruns CJ. Vascular endothelial growth factor in esophageal cancer. J Surg Oncol 2004;87:95–104.

[19] Takahashi Y, Kitadai Y, Bucana CD, Cleary KR, Ellis LM. Expression of vascular endothelial growth factor and its receptor, KDR, correlates with vascularity, metastasis, and proliferation of human colon cancer. Cancer Res 1995;55:3964–3968.

[20] Toi M, Inada K, Suzuki H, Tominaga T. Tumor angiogenesis in breast cancer: its importance as a prognostic indicator and the association with vascular endothelial growth factor expression. Breast Cancer Res Treat 1995;36:193–204.

[21] Torimura T, Sata M, Ueno T, Kin M, Tsuji R, Suzaku K, et al. Increased expression of vascular endothelial growth factor is associated with tumor progression in hepatocellular carcinoma. Hum Pathol 1998;29:986–991.

[22] Amaoka N, Osada S, Kanematsu M, Imai H, Tomita H, Tokuyama Y, et al. Clinicopathological features of hepatocellular carcinoma evaluated by vascular endothelial growth factor expression. J Gastroenterol Hepatol 2007;22:2202–2207.

[23] Park YN, Kim YB, Yang KM, Park C. Increased expression of vascular endothelial growth factor and angiogenesis in the early stage of multistep hepatocarcinogenesis. Arch Pathol Lab Med 2000;124:1061–1065.

[24] Yamaguchi R, Yano H, Nakashima O, Akiba J, Nishida N, Kurogi M, et al. Expression of vascular endothelial growth factor-C in human hepatocellular carcinoma. J Gastroenterol Hepatol 2006;21:152–160.

[25] Yamaguchi R, Yano H, Iemura A, Ogasawara S, Haramaki M, Kojiro M. Expression of vascular endothelial growth factor in human hepatocellular carcinoma. Hepatology 1998;28:68–77.

[26] Amaoka N, Saio M, Nonaka K, Imai H, Tomita H, Sakashita F, et al. Expression of vascular endothelial growth factor receptors is closely related to the histological grade of hepatocellular carcinoma. Oncol Rep 2006;16:3–10.

[27] Stroescu C, Dragnea A, Ivanov B, Pechianu C, Herlea V, Sgarbura O, et al. Expression of p53, Bcl-2, VEGF, Ki67 and PCNA and prognostic significance in hepatocellular carcinoma. J Gastrointestin Liver Dis 2008;17:411–417.

[28] Amann T, Maegdefrau U, Hartmann A, Agaimy A, Marienhagen J, Weiss TS, et al. GLUT1 expression is increased in hepatocellular carcinoma and promotes tumorigenesis. Am J Pathol 2009;174:1544–1552.

Author's personal copy

[29] Narita M, Hatano E, Arizono S, Miyagawa-Hayashino A, Isoda H, Kitamura K, et al. Expression of OATP1B3 determines uptake of Gd-EOB-DTPA in hepatocellular carcinoma. J Gastroenterol 2009;44:793–798.
[30] Seo S, Hatano E, Higashi T, Nakajima A, Nakamoto Y, Tada M, et al. P-glycoprotein expression affects 18F-fluorodeoxyglucose accumulation in hepatocellular carcinoma in vivo and in vitro. Int J Oncol 2009;34: 1303–1312.
[31] Mamede M, Higashi T, Kitaichi M, Ishizu K, Ishimori T, Nakamoto Y, et al. [18F] FDG uptake and PCNA, GLUT-1, and hexokinase-II expressions in cancers and inflammatory lesions of the lung. Neoplasia 2005;7:369–379.
[32] Lee TK, Poon RT, Yuen AP, Ling MT, Wang XH, Wong YC, et al. Regulation of angiogenesis by Id-1 through hypoxia-inducible factor-1alpha-mediated vascular endothelial growth factor up-regulation in hepatocellular carcinoma. Clin Cancer Res 2006;12:6910–6919.
[33] Kolev Y, Uetake H, Iida S, Ishikawa T, Kawano T, Sugihara K. Prognostic significance of VEGF expression in correlation with COX-2, microvessel density, and clinicopathological characteristics in human gastric carcinoma. Ann Surg Oncol 2007;14:2738–2747.
[34] Birner P, Schindl M, Obermair A, Plank C, Breitenecker G, Oberhuber G. Overexpression of hypoxia-inducible factor 1alpha is a marker for an unfavorable prognosis in early-stage invasive cervical cancer. Cancer Res 2000;60:4693–4696.
[35] Soumaoro LT, Uetake H, Higuchi T, Takagi Y, Enomoto M, Sugihara K. Cyclooxygenase-2 expression: a significant prognostic indicator for patients with colorectal cancer. Clin Cancer Res 2004;10:8465–8471.
[36] Poon RT, Lau CP, Ho JW, Yu WC, Fan ST, Wong J. Tissue factor expression correlates with tumor angiogenesis and invasiveness in human hepatocellular carcinoma. Clin Cancer Res 2003;9:5339–5345.
[37] Higashi T, Hatano E, Ikai I, Nishii R, Nakamoto Y, Ishizu K, et al. FDG PET as a prognostic predictor in the early post-therapeutic evaluation for unresectable hepatocellular carcinoma. Eur J Nucl Med Mol Imaging 2009;37: 468–482.
[38] Oakman C, Santarpia L, Di Leo A. Breast cancer assessment tools and optimizing adjuvant therapy. Nat Rev Clin Oncol 2010;7:725–732.
[39] Wiesner FG, Magener A, Fasching PA, Wesse J, Bani MR, Rauh C, et al. Ki-67 as a prognostic molecular marker in routine clinical use in breast cancer patients. Breast 2009;18:135–141.
[40] Jung SY, Han W, Lee JW, Ko E, Kim E, Yu JH, et al. Ki-67 expression gives additional prognostic information on St. Gallen 2007 and Adjuvant! Online risk categories in early breast cancer. Ann Surg Oncol 2009;16:1112–1121.
[41] Llovet JM, Di Bisceglie AM, Bruix J, Kramer BS, Lencioni R, Zhu AX, et al. Design and endpoints of clinical trials in hepatocellular carcinoma. J Natl Cancer Inst 2008;100:698–711.
[42] Thorens B. Molecular and cellular physiology of GLUT-2, a high-Km facilitated diffusion glucose transporter. Int Rev Cytol 1992;137:209–238.
[43] Tal M, Schneider DL, Thorens B, Lodish HF. Restricted expression of the erythroid/brain glucose transporter isoform to perivenous hepatocytes in rats. Modulation by glucose. J Clin Invest 1990;86:986–992.
[44] Christofk HR, Vander Heiden MG, Harris MH, Ramanathan A, Gerszten RE, Wei R, et al. The M2 splice isoform of pyruvate kinase is important for cancer metabolism and tumour growth. Nature 2008;452:230–233.
[45] Christofk HR, Vander Heiden MG, Wu N, Asara JM, Cantley LC. Pyruvate kinase M2 is a phosphotyrosine-binding protein. Nature 2008;452: 181–186.
[46] Tani K, Yoshida MC, Satoh H, Mitamura K, Noguchi T, Tanaka T, et al. Human M2-type pyruvate kinase: cDNA cloning, chromosomal assignment and expression in hepatoma. Gene 1988;73:509–516.
[47] Hamaguchi T, Iizuka N, Tsunedomi R, Hamamoto Y, Miyamoto T, Iida M, et al. Glycolysis module activated by hypoxia-inducible factor 1alpha is related to the aggressive phenotype of hepatocellular carcinoma. Int J Oncol 2008;33:725–731.
[48] Uematsu S, Higashi T, Nouso K, Kariyama K, Nakamura S, Suzuki M, et al. Altered expression of vascular endothelial growth factor, fibroblast growth factor-2 and endostatin in patients with hepatocellular carcinoma. J Gastroenterol Hepatol 2005;20:583–588.
[49] Zacharoulis D, Hatzitheofilou C, Athanasiou E, Zacharoulis S. Antiangiogenic strategies in hepatocellular carcinoma: current status. Expert Rev Anticancer Ther 2005;5:645–656.
[50] Kanematsu M, Osada S, Amaoka N, Goshima S, Kondo H, Kato H, et al. Expression of vascular endothelial growth factor in hepatocellular carcinoma and the surrounding liver and correlation with MRI findings. AJR Am J Roentgenol 2005;184:832–841.
[51] Semenza GL. Defining the role of hypoxia-inducible factor 1 in cancer biology and therapeutics. Oncogene 2010;29:625–634.
[52] Nijkamp MW, van der Bilt JD, de Bruijn MT, Molenaar IQ, Voest EE, van Diest PJ, et al. Accelerated perinecrotic outgrowth of colorectal liver metastases following radiofrequency ablation is a hypoxia-driven phenomenon. Ann Surg 2009;249:814–823.
[53] Findlay M, Young H, Cunningham D, Iveson A, Cronin B, Hickish T, et al. Noninvasive monitoring of tumor metabolism using fluorodeoxyglucose and positron emission tomography in colorectal cancer liver metastases: correlation with tumor response to fluorouracil. J Clin Oncol 1996;14:700–708.
[54] Miles KA, Williams RE. Warburg revisited: imaging tumour blood flow and metabolism. Cancer Imaging 2008;8:81–86.
[55] Pelicano H, Martin DS, Xu RH, Huang P. Glycolysis inhibition for anticancer treatment. Oncogene 2006;25:4633–4646.